Acetylation of MORC2 by NAT10 regulates cell-cycle checkpoint control and resistance to DNA-damaging chemotherapy and radiotherapy in breast cancer

Hong-Yi Liu[1],[†], Ying-Ying Liu[1,2,3,4],[†], Fan Yang[1,2,3,4], Lin Zhang[1,2], Fang-Lin Zhang[1,2], Xin Hu[1,2,3,4,5],[*], Zhi-Min Shao[1,2,3,4,5],[*] and Da-Qiang Li ⊙[1,2,3,4,5,6],[*]

[1]Fudan University Shanghai Cancer Center and Shanghai Key Laboratory of Medical Epigenetics, Institutes of Biomedical Sciences, Fudan University, Shanghai 200032, China, [2]Cancer Institute, Shanghai Medical College, Fudan University, Shanghai 200032, China, [3]Department of Oncology, Shanghai Medical College, Fudan University, Shanghai 200032, China, [4]Department of Breast Surgery, Shanghai Medical College, Fudan University, Shanghai 200032, China, [5]Shanghai Key Laboratory of Breast Cancer, Shanghai Medical College, Fudan University, Shanghai 200032, China and [6]International Co-laboratory of Medical Epigenetics and Metabolism, Ministry of Science and Technology, Shanghai 200032, China

ABSTRACT

MORC family CW-type zinc finger 2 (MORC2) is an oncogenic chromatin-remodeling enzyme with an emerging role in DNA repair. Here, we report a novel function for MORC2 in cell-cycle checkpoint control through an acetylation-dependent mechanism. MORC2 is acetylated by the acetyltransferase NAT10 at lysine 767 (K767Ac) and this process is counteracted by the deacetylase SIRT2 under unperturbed conditions. DNA-damaging chemotherapeutic agents and ionizing radiation stimulate MORC2 K767Ac through enhancing the interaction between MORC2 and NAT10. Notably, acetylated MORC2 binds to histone H3 phosphorylation at threonine 11 (H3T11P) and is essential for DNA damage-induced reduction of H3T11P and transcriptional repression of its downstream target genes *CDK1* and *Cyclin B1*, thus contributing to DNA damage-induced G2 checkpoint activation. Chemical inhibition or depletion of NAT10 or expression of an acetylation-defective MORC2 (K767R) forces cells to pass through G2 checkpoint, resulting in hypersensitivity to DNA-damaging agents. Moreover, MORC2 acetylation levels are associated with elevated NAT10 expression in clinical breast tumor samples. Together, these findings uncover a previously unrecognized role for MORC2 in regulating DNA damage-induced G2

checkpoint through NAT10-mediated acetylation and provide a potential therapeutic strategy to sensitize breast cancer cells to DNA-damaging chemotherapy and radiotherapy by targeting NAT10.

INTRODUCTION

The DNA damage response plays a central role in the onset of human cancer and tumor responses to DNA-damaging chemotherapy and radiotherapy (1,2). A common cellular response to genotoxic stress is activation of a cell cycle checkpoint, which blocks cell-cycle progression and allows time to repair DNA lesions before cells reenter the normal cell cycle (3). Eukaryotic cells have three major DNA damage checkpoints, including the G1/S, intra-S-phase, and G2/M checkpoints (4). The G1/S checkpoint is mainly propagated through the activation of the p53 pathway. As the p53 gene is frequently mutated or silenced in human cancer (5,6), most cancer cells have a dysfunctional G1/S checkpoint and therefore depend on the S and G2/M checkpoints for survival in response to genotoxic stress (7). The intra-S phase checkpoint serves to address both DNA replication errors and DNA damage incurred during S phase, which is controlled by the ataxia telangiectasia and Rad3 related (ATR)/checkpoint kinase 1 (CHK1) signaling (8). The G2/M checkpoint restricts mitosis onset in response to genotoxic stress, and its deregulation allows cells with damaged DNA to proceed into the mitosis phase, leading to chromosome instability that is linked to tumorigenesis, mitotic catastrophe, or cell death (9). Cyclin-dependent kinase 1 (CDK1) and its interactor Cyclin B1

are key regulators for the G2/M transition and mitotic progression ([10](ref)). When DNA damage occurs in late S or the G2 phase, the CDK1/Cyclin B1 complex is inactivated, at either transcriptional or posttranslational level, to arrest cells at the G2/M transition ([9,10](ref)). Interestingly, it has recently been shown that DNA damage rapidly reduces histone H3 threonine 11 phosphorylation (H3T11P), a novel chromatin mark for transcriptional activation ([11](ref)), through activating protein phosphatase 1γ (PP1γ) ([12](ref)) or releasing CHK1 kinase from chromatin ([13](ref)). Decreased H3T11P contributes to transcriptional repression of CDK1 and Cyclin B1 through reducing histone H3 acetylation at lysine 9 (H3K9Ac) at their promoters in response to DNA damage ([13](ref)). Although the basic framework of cell-cycle checkpoints in eukaryotic cells has been outlined, it remains to identify new players that regulate this complex network.

ATP-dependent chromatin remodeling enzymes are key players in all DNA-templated reactions in eukaryotes, and their deregulation is intimately implicated in various human diseases including cancer ([14](ref)). One such key enzyme is the MORC family CW-type zinc finger 2 (MORC2), a member of the highly conserved microrchidia (MORC) family of ATPases ([15–17](ref)). Being a characteristic of MORC proteins, MORC2 contains an N-terminal catalytically active ATPase module and a central CW-type zinc finger (CW-ZF) domain ([16,18,19](ref)). The ATPase module of MORC2 is composed of a gyrase, Hsp90, histidine kinase, and MutL (GHKL) domain and a S5-fold domain ([15,20](ref)), and its ATPase activity is critical for epigenetic gene silencing ([18,19](ref)) and DNA damage repair ([21](ref)). Notably, mutations in the ATPase module of MORC2 have been mechanistically linked to hereditary Charcot-Marie-Tooth disease ([18,22–25](ref)) and triple-negative breast cancer ([26](ref)). The CW-ZF domain is structurally similar to the plant homeo domain (PHD) finger and acts as a histone recognition module for trimethylation of histone H3 at lysine 4 (H3K4me3) in multiple chromatin-associated proteins ([27–29](ref)). Strikingly, MORC2 is unable to bind to H3K4me3 mark due to the absence of an aromatic cage in its CW-ZF domain ([30](ref)), indicating that MORC2 engages with chromatin *via* distinct mechanisms. In addition, MORC2 contains a unique C-terminal chromo-like domain that is absent in other MORCs and four dispersed coiled-coil domains ([16](ref)), but their biological functions remain uncharacterized. Recent studies from our laboratory and others indicate that MORC2 is frequently overexpressed in multiple types of human cancer and acts as a driver of oncogenesis ([26,31–35](ref)). In addition, we recently demonstrated that MORC2 is a DNA damage-responsive protein with an emerging role in DNA repair ([21,36](ref)). However, its functional and mechanistic role in cell-cycle checkpoint control remains unexplored.

Emerging evidence shows that lysine acetylation of histones and nonhistone proteins acts as a key player in cellular response to DNA damage ([37](ref)). Protein acetylation is controlled by the concerted action of lysine acetyltransferases (KATs) and lysine deacetylases (KDACs), which catalyze the addition and removal of acetyl groups on lysine residues, respectively ([38,39](ref)). To date, 22 KATs and 18 KDACs have been identified in human genome ([39](ref)). According to their structure and catalytic mechanism, KATs can be grouped into three major families, including GCN5-related N-acetyltransferase (GNAT), CBP/p300, and MYST, while KDACs are classified into two distinct families, including Zn^{2+}-dependent histone deacetylases (HDAC1-11) and NAD^+-dependent sirtuin deacetylases (SIRT1-7) ([39](ref)). N-acetyltransferase 10 (NAT10) is a member of the GNAT family of KATs and has been documented to acetylate RNA ([40–42](ref)), transcriptional factor p53 ([43](ref)), transcriptional cofactor Che-1 ([44](ref)), and α-tubulin ([45](ref)). Moreover, deregulation of NAT10 has been implicated in Hutchinson-Gilford progeria syndrome ([46–48](ref)) and several types of human cancer ([45,49–51](ref)). More recently, we demonstrated that NAT10 acetylates poly(ADP-ribose) polymerase 1 (PARP1), a key DNA repair protein, and is a potential binding partner for MORC2 ([36](ref)). However, whether MORC2 is a novel substrate of NAT10 remains unknown.

In this study, we report that NAT10 directly acetylates MORC2 at the conserved lysine 767 (K767Ac), which is antagonized by SIRT2 under unstressed conditions. Moreover, MORC2 K767Ac is stimulated by DNA-damaging agents in a NAT10, but not SIRT2, dependent manner, and is critical for G2 checkpoint arrest through transcriptional repression of H3T11P-mediated CDK1 and Cyclin B1. Consequently, chemical inhibition or depletion of NAT10 or expression of an acetylation-deficient mutant MORC2 results in hypersensitivity to DNA-damaging therapeutic agents. These findings establish the importance and regulatory mechanism of MORC2 acetylation in governing DNA damage checkpoint signaling and therapeutic resistance, and motivate the combined use of NAT10 inhibitor Remodelin and conventional DNA-damaging chemotherapy and radiotherapy to optimize clinical outcome of patients with breast cancer.

MATERIALS AND METHODS

Cell cultures and treatments

Human breast cancer MCF-7 (#SCSP-531), T47D (#TCHu 87), BT549 (#TCHu 93) cell lines and human embryonic kidney HEK293T cell line (#SCSP-502) were obtained from the Cell Bank of the Chinese Academy of Sciences (Shanghai, China), and were authenticated by detection of mycoplasma, DNA-fingerprinting, and cell vitality. Cells were maintained in DMEM (BasalMedia, #L110) media supplemented with 10% fetal bovine serum (ExCell Bio, #FSP500) and 1× penicillin-streptomycin solution (BasalMedia, #S110B). Exponentially growing cells were irradiated with γ-rays using a ^{137}Cs Gammacell-40 irradiator (Institute of Radiation Medicine, Fudan University) at room temperature. After incubation for the indicated times, cells were harvested for further experiments. Control cells were identically processed but not irradiated. The detailed information for chemical inhibitors is provided in Supplementary Table S1. Unless otherwise stated, all reagents were purchased from Sigma-Aldrich.

Clinical samples

Written informed consent was obtained from all patients, and the protocol of this study was approved by the institutional ethics review board of Fudan University Shanghai Cancer Center. A total of 16 pairs of primary breast

tumor tissues and adjacent normal breast tissues and 128 primary breast cancer specimens were obtained from breast cancer patients who underwent surgery at Fudan University Shanghai Cancer Center. All specimens were confirmed by pathologic diagnosis. No patients received chemotherapy or radiotherapy before surgery. Characterization of clinic-pathological features of 128 breast cancer patients is described in Supplementary Table S2.

Expression vectors, plasmid transfection and lentiviral infection

Myc-DDK-tagged MORC2 (#RC200518) and GFP-tagged NAT10 (#RG207082) cDNAs were obtained from Origene. Flag-His-NAT10 (#CH874058) cDNA was purchased from Vigene Biosciences. HA-SIRT1 and HA-SIRT2 expression vectors were kindly provide by Dr. Hai-Xin Yuan (Fudan MCB laboratory, Shanghai) (52). LentiCas9-Blast (Addgene, #52962) and lentiGuide-Puro (Addgene, #52963) vectors were provided by Feng Zhang laboratory. Molecular cloning was performed using either ClonExpress Ultra One Step Cloning Kit (Vazyme, #C115-02) or CloneEZ PCR Cloning Kit (Genscript, #L00339). Amino-acid substitutions and the deletion mutants were generated by PCR-based methods. All construct sequences were verified by DNA sequencing. The detailed information concerning expression constructs and the primers used for molecular cloning is provided in Supplementary Tables S3 and S4.

Transient plasmid transfection was performed using Neofect DNA transfection reagent (TengyiBio, #TF201201) according to the manufacturer's protocol. Lentiviral infection and generation of stable cell lines were carried out as described previously (26,53). The NAT10, SIRT2, and PARP1 KO cell lines were generated using the CRISPR/Cas9 system (54), and were validated by immunoblotting analysis and Sanger sequencing. The individual gRNA sequences are provided in Supplementary Table S5.

siRNAs and transfection

The siRNAs targeting NAT10, SIRT2, and corresponding negative control siRNAs (siNC) were purchased from GenePharma (Shanghai, China). The siRNA target sequences are listed in Supplementary Table S6. The siRNA duplexes were transfected into cells using Lipofectamine 2000 transfection reagents (Invitrogen, #2041726) following the manufacturer's instructions. Knockdown efficiency was validated by immunoblotting after 48 h of transfection.

Antibodies, immunoblotting, and immunoprecipitation assays

All of the primary and secondary antibodies used in this study are summarized in Supplementary Table S7. The MORC2 767Ac antibody was generated commercially from immunizing rabbits at Hebu Biotech (Shanghai, China). The sequence of peptide used to immunize rabbits is as follows: RGRFVV[acetyl-Lys]EEKKDSN. Immunoblotting analysis and IP assays were performed as described previously (26,53). The optical density of immunoblotting bands

was quantified using ImageJ program and was normalized to the internal control Vinculin.

Purification of recombinant proteins

The GST-tagged constructs in pGEX-6P-1 vector and His-tag constructs in pET-28a vector were transformed into *E. coli* strain BL21 (DE3) and incubated with 0.2 mM IPTG (Invitrogen, #15529019) to induce expression of recombination proteins at 16°C overnight. GST-tag proteins were purified using Glutathione Sepharose 4B beads (GE Healthcare, #17075601),while His-tag proteins were purified using Ni-NTA agarose (TIANGEN Biotech, #WM6-45-655-101), following the manufacturer's instructions. The purified proteins were immediately used for the experiments or frozen at −80°C.

Histone peptide pull-down assays

The Biotin-labeled histone H3 phosphorylation at T11 peptide (biotin-ARTKQTARKS(pThr)GGKAPRKQLA) and the unmodified control peptide (biotin-ARTKQTARKS TGGKAPRKQLA) were chemically synthesized at Sangon Biotech (Shanghai, China). Biotinylated peptides were immobilized on Streptavidin sepharose beads (GE Healthcare, #17-5113-01) and then incubated with purified His-MORC2 protein. Reciprocally, purified His-MORC2 proteins were immobilized on Ni-NTA agarose beads (TIANGEN Biotech, #WM6-45-655-101) and then incubated biotinylated peptides. Bound proteins were resolved by SDS-PAGE and detected by immunoblotting with the indicated antibodies.

In vitro acetylation and deacetylation assays

For *in vitro* acetylation assays, His-MORC2 protein was purified using Ni-NTA agarose and then incubated with recombinant NAT10 (Origene, #TP307082) in the HAT buffer (50 mM Tris–HCl, pH 8.0, 50 mM NaCl, 4 mM MgCl$_2$, 0.1 mM EDTA, 1 mM DTT and 10% glycerol) in the presence or the absence of 2 mM acetyl-coenzyme A (acetyl-CoA; Sigma, #A2056) at 37°C for 1 h. For *in vitro* deacetylation assays, acetylated MORC2 was incubated with recombinant human SIRT2 protein (Origene, #AR09743PU) in the presence of 5 mM NAD$^+$ at 37°C for 1 h. The beads were washed three times with HAT buffer and the reaction was terminated by the addition of 2× SDS loading buffer. Acetylation of MORC2 was detected by immunoblotting with an anti-K767Ac antibody.

Histone binding assay

The MODified Histone Peptide Arrays containing 384 unique histone modification combinations in duplicate were purchased from Active Motif (#13005). Flag-MORC2 K767R and Flag-MORC2 K767Q proteins were purified from HEK293T cells using Flag M2 agarose beads (Sigma, #F2426) and then eluted by DYKDDDDK synthetic peptide (Sino Biol, #PP101274). Histone binding assays were performed according to the manufacturer's instructions. Briefly, each array was blocked in 3 ml blocking solution

(5% BSA) for 2 h, washed with TTBS (10 mM Tris–HCl, pH7.4, 0.05% Tween 20, 150 mM NaCl) once, and then incubated with purified MORC2 proteins in protein-binding buffer (0.5% NP40 buffer) at 4°C for 3 h. The arrays were washed three times with TTBS, and then incubated with an anti-Flag or anti-Myc antibody (positive control) at 4°C overnight. After washing three times with TTBS, HRP-linked anti-mouse second antibody was added. After washing three times with TTBS, signals were detected by ECL visualization and analyzed by Array Analysis Software.

qPCR and ChIP-qPCR

Total RNA was extracted using TRIzol agent (Invitrogen, #15596018) and subjected to cDNA synthesis using Prime-Script RT Master Mix (Takara, #RR036). qPCR was performed using SYBR Premix Ex Taq (Tli RNaseH Plus) (Takara, #RR420) following the manufacturer's instructions. All data was normalized to the housekeeping gene β-actin, and quantitative measures were obtained using the comparative CT method. Primers used for qPCR are listed in Supplementary Table S8. ChIP assays were performed using a SimpleChIP Plus Sonication Chromatin IP Kit (Cell Signaling Technology, #56383) according to the manufacturer's instructions. All data was displayed as corresponding fold change and anti-rabbit IgG was regarded as a negative control. The primer pairs used for ChIP analysis are listed in Supplementary Table S8.

Flow cytometry analysis

A total of 1×10^6 cells were fixed using 70% pre-cooled ethanol at 4°C overnight, then washed with PBS, and then subjected to cell-cycle analysis using Cell Cycle and Apoptosis Analysis Kit (Yeasen, #40301ES60) following the manufacturer's instructions. Cell cycle data were acquired on Beckman Cytomics FC 500 BD FACSCanto II and were analyzed by FlowJov10 software.

To distinguish cells in G2 or M phase, cells were treated with or without 10 Gy of IR. After 24 h of treatment, cells were fixed in 70% ethanol overnight and washed with PBS. Then, cells were incubated with an anti-mitotic protein antibody [MPM-2] (Abcam, #ab14581) in IFA-Tx buffer (4% FCS, 150 nM NaCl, 10 nM HEPES, 0.1% sodium azide, 0.1% Triton X-100) at room temperature for 1 h. Cells were washed and incubated with anti-mouse FITC-conjugated secondary antibody in IFA-Tx buffer for 1 h at room temperature in darkness. Finally, cells were washed and resuspended in 1 ml of PBS for 30 min in the dark. MPM-2 positive cells were delected by Flow cytometry.

Colony formation survival and CCK-8 assays

A total of 5×10^3 cells were seeded into 12-well plate (colony formation survival assay) or 96-well plates (CCK-8 assay) in triplicates overnight, treated with IR or the indicated drugs. For colony formation assays, cells were fixed after 10 days of treatment by methanol, stained with 0.2% crystal violet solution and photographed. Colonies consisting of >50 cells were counted. For CCK-8 assays, after 48 h of treatment, 10 μl CCK-8 solution (Yeasen, #40203ES60)

was added to each well. The plates were incubated in an incubator for 3 h, and then absorbance at 450 nm was determined.

Immunofluorescent staining

Immunofluorescent staining was carried out as described previously (26,53). Briefly, cells were fixed with 4% methanol-free formaldehyde (Yeasen, #36314ES76) for 20 min and permeabilized with 0.5% Triton X-100 for 20 min at 4°C. After rinsing with PBS for three times, cells were blocked for 1 h with 5% goat serum and incubated with an anti-K767Ac (1:200), anti-γH2AX (1:500), anti-HA (1:500), or anti-Flag (1:500) antibody in 5% goat serum overnight at 4°C. Cells were rinsed with PBS three times and incubated with the secondary antibodies conjugated with Alexa 488 or Alexa-568 (1:500) at room temperature for 1 h. Then, cells were washed with PBS three times, and sealed with DAPI-containing fluoroshield mounting medium (Abcam, #ab104139). Images were visualized with Leica SP5 confocal microscope and analyzed.

Immunohistochemical staining

A total of 128 primary breast cancer specimens were obtained from the Department of Pathology, Fudan University Shanghai Cancer Center. IHC staining was performed as previously described (55). The anti-NAT10 (Abcam, ab194297, 1:150) and anti-MORC2 K767Ac (1:50) primary antibodies were used. The representative photographs were taken using Olympus BX43 microscope. Interpretation of the IHC results was performed by two independent pathologists who were blinded to the clinicopathological information. Slides were evaluated using light microscopy and a standard semi-quantitative immunoreactivity score as described previously (56). By recording the percentage of positive staining (0 = negative, 1 ≤ 10%, 2 = 10–50%, 3 ≥ 50%) and staining intensity (0 = no, 1 = weak, 2 = moderate, 3 = strong) for each sample, immunoreactivity score (IRS) (0-9) was calculated by multiplying positive staining percentage with staining intensity. Low and high expression were defined according to the median IRS.

Statistical analysis

All data is presented as the mean ± standard deviation from at least three independent experiments. The unpaired two-tailed Student's *t* test was used to compare data between two groups using SPSS20. Correlation coefficients were calculated using the *Pearson* test. *P* values less than 0.05 were considered statistically significant.

RESULTS

MORC2 is acetylated at the evolutionarily conserved lysine 767

To examine whether MORC2 is modified by acetylation, human breast cancer MCF-7, T47D, and BT549 cells were treated with trichostatin A (TSA), an inhibitor for classic HDACs, and nicotinamide (NAM), a SIRT family inhibitor, to block the action of KDACs during the experiments. As a positive control, treatment with TSA and NAM
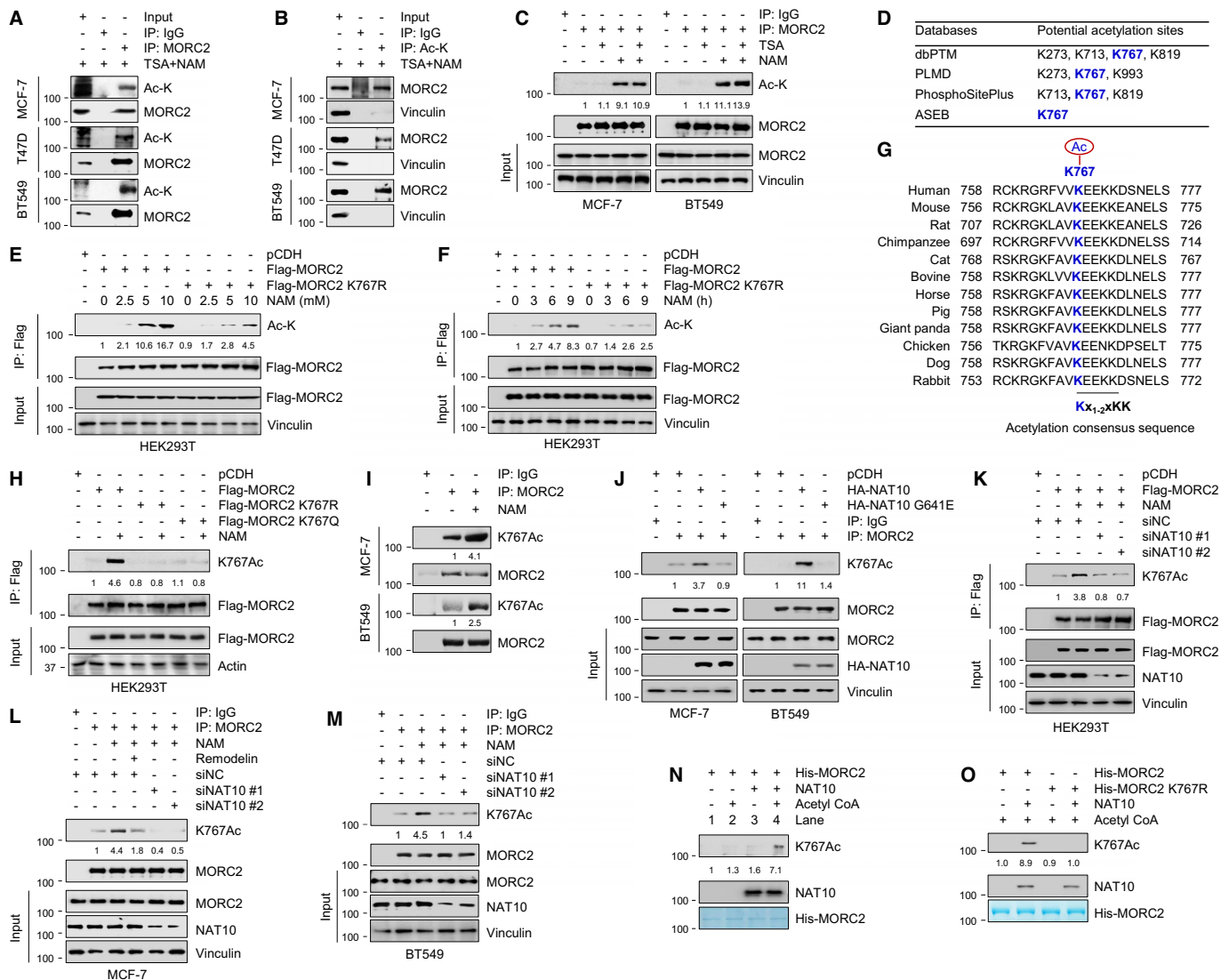
Figure 1. NAT10 acetylates MORC2 at K767. (**A**, **B**) Cells were treated with 5 μM TSA and 5 mM NAM for 6 h. Lysates were subjected to IP assays with control IgG, an anti-MORC2 (A) or anti-Ac-K (B) antibody, followed by immunoblotting analysis with the indicated antibodies. (**C**) Cells were treated with or without 5 mM NAM or 5 μM TSA alone or in combination for 6 h and subjected to IP and immunoblotting analysis with the indicated antibodies. MORC2 acetylation levels were normalized to those of total MORC2 protein. (**D**) Analysis of MORC2 acetylation sites in publicly available databases. (**E**, **F**) HEK293T cells stably expressing pCDH, Flag-MORC2, and Flag-MORC2 K767R were treated or without NAM at the indicated concentrations for 6 h (E) or 5 mM NAM for the indicated times (F). IP and immunoblotting analyses were performed with the indicated antibodies. (**G**) Alignment of MORC2 protein sequence across different species. (**H**) HEK293T cells stably expressing pCDH and Flag-MORC2 (WT, K767R and K767Q) were treated with or without 5 mM NAM for 6 h and subjected to IP and immunoblotting analyses with the indicated antibodies. (**I**) MCF-7 and BT549 cells were treated with or without 5 mM NAM for 6 h and subjected to IP and immunoblotting analyses with the indicated antibodies. MORC2 K767Ac levels were normalized to those of total MORC2 protein. (**J**) MCF-7 and BT549 cells were transfected with pCDH, HA-NAT10, or HA-NAT10 G641E. After 48 h of transfection, lysates were subjected to IP and immunoblotting analysis. (**K–M**) HEK293T cells stably expressing pCDH and Flag-MORC2 (K), MCF-7 (L), or BT549 (M) cells were transfected with negative control siRNA (siNC) or two siRNAs targeting NAT10 (siNAT10). After 48 h of transfection, cells with treated with or without 5 mM NAM for 6 h and subjected to IP and immunoblotting analysis. In L, cells were pretreated with or without 5 μM Remodelin for 3 h prior to NAM treatment. (**N**) Purified His-MORC2 was incubated with or without purified NAT10, 2 mM acetyl-CoA in reaction buffer at 37°C for 1 h. MORC2 K767Ac was detected by immunoblotting. His-MORC2 was visualized by Coomassie blue staining. (**O**) Purified His-MORC2 (WT and K767R) were incubated with or without purified NAT10, 2 mM acetyl-CoA in reaction buffer at 37°C for 1 h. MORC2 K767Ac was detected by immunoblotting. His-MORC2 was visualized by Coomassie blue staining.

resulted in an increase in levels of global lysine acetylation and histone H3 acetylation at lysine 56 (H3K56Ac) in a dose- and time-dependent manner (Supplementary Figure S1A and S1B). Reciprocal IP assays using an anti-MORC2 or anti-acetylated lysine (Ac-K) antibody revealed that endogenous MORC2 was indeed acetylated (Figure 1A and B). To validate these results, we repeated this experiment with Vorinostat (SAHA), a HDAC inhibitor, and Sirtinol, a SIRT1/2 inhibitor (57). IP assays using an anti-Ac-K antibody obtained the similar results (Supplementary Figure S1C). In addition, acetylation of ectopically expressed Flag-MORC2 in HEK293T cells was demonstrated by IP and immunoblotting analysis with an anti-Flag or anti-Ac-K antibody (Supplementary Figure S1D). Further studies showed that treatment with NAM, but not TSA, enhanced exogenous and endogenous MORC2 acetylation (Figure 1C and Supplementary Figure S1E), indicating that member(s) of SIRT family may be involved in MORC2 deacetylation.

To identify the acetylation site of MORC2, we first analyzed publicly available PTM databases, including database for PTM (dbPTM) (58), protein lysine modification database (PLMD) (59), PhosphoSitePlus (60), and acetylation set enrichment based (ASEB) program (61), and found five potential acetylation sites (K273, K713, K767, K819 and K993) (Figure 1D). To verify these results, we substituted the five lysine (K) resides with nonacetylable arginine (R) individually and examined their acetylation status in the presence or absence of NAM. Results showed that the K767R mutation significantly reduced NAM-induced upregulation of MORC2 acetylation compared to its wild-type (WT) counterpart and other four substitution mutations (Supplementary Figure S1F). Consistently, treatment with NAM significantly enhanced acetylation of WT MORC2 in comparison with K767R mutant MORC2 (Figure 1E and F). These results suggest that the K767 is the major acetylation site of MORC2. Notably, K767 acetylation in MORC2 has recently been documented in several acetylome proteomic studies (62–64). Sequence alignment revealed that the K767 residue is highly conserved across species and is embedded within an acetylation consensus sequence $Kx_{1-2}xKK$ (amino acids 767–771: KEEKK) (Figure 1G).

To further confirm these results, we generated a specific antibody against acetylated MORC2 at K767 using an acetylated peptide antigen (RGRFVV[acetyl-K]EEKK DSN). Dot blot assays showed that the K767Ac antibody specifically recognized the K767 acetylated peptide, but not the unmodified control (Supplementary Figure S1G). Moreover, NAM treatment enhanced K767Ac of WT MORC2, but not either K767R or K767Q (acetylation-mimic mutation) mutant (Figure 1H). Moreover, treatment of MCF-7 and BT549 cells with NAM significantly enhanced endogenous MORC2 K767Ac (Figure 1I). Together, these results indicate that MORC2 is primarily acetylated at K767.

NAT10 is the major acetyltransferase for MORC2 K767Ac

Upon examination of potential KATs responsible for MORC2 K767Ac, our attention was drawn to NAT10, which is a potential binding partner of MORC2 revealed by our recent proteomic analysis (36). To validate whether MORC2 interacts with NAT10, HEK293T cells were transfected with Flag-MORC2, HA-NAT10 alone or in combination, and subjected to reciprocal IP assays with an anti-Flag or anti-HA antibody. Immunoblotting analysis revealed that Flag-MORC2 and HA-NAT10 pulled down each other when co-expressed only (Supplementary Figure S2A). Moreover, there was an interaction between MORC2 and NAT10 at the endogenous level in MCF-7 and BT549 cells (Supplementary Figure S2B). GST pull-down assays showed that GST-NAT10 bound to His-MORC2 (Supplementary Figure S2C), while GST-MORC2 interacted with His-NAT10 (Supplementary Figure S2D), indicating a direct interaction between both proteins. These results indicate that NAT10 interacts with MORC2 both *in vitro* and *in vivo*.

As NAT10 is a novel KAT with intrinsic acetyltransferase activities (40–45), we next investigated whether NAT10 acetylates MORC2. Results showed that ectopic expression of WT NAT10, but not its catalytically inactive mutant (G641E) (48), enhanced K767Ac of exogenously expressed MORC2 in HEK293T cells (Supplementary Figure S2E) and of endogenous MORC2 in MCF-7 and BT549 cells (Figure 1J). Conversely, knockdown of NAT10 using two independent siRNAs reduced K767Ac of exogenous (Figure 1K) and endogenous (Figure 1L and M) MORC2. In support of these findings, inhibition of NAT10 activity by the small molecule inhibitor Remodelin (48) reduced MORC2 K767Ac (Figure 1L and Supplementary Figure S2F). *In vitro* acetylation assays using purified His-MORC2 and recombinant NAT10 proteins demonstrated that NAT10 efficiently acetylated WT but not the K767R mutant MORC2 (Figure 1N and O), further confirming that K767 of MORC2 is the primary acetylation site by NAT10. As a negative control, we did not observe a reactive signal in the absence of acetyl-CoA or recombinant NAT10 (Figure 1N, compare lanes 2 and 3 with 4). Collectively, these results suggest that NAT10 directly interacts with MORC2 and acetylates it at K767.

SIRT2 deacetylates MORC2 at K767

Lysine acetylation is a dynamic process that can be reversed by specific KDAC(s). The above results indicate the SIRT family of KDACs may be preferentially involved in MORC2 deacetylation (Figure 1C and Supplementary Figure S1E). Among 7 SIRT proteins in mammals, only SIRT1-3 have robust deacetylase activity, while SIRT4-7 have either no detectable or very weak deacetylase activity (65). In addition, SIRT1 and SIRT2 are localized in both nuclear and cytoplasm in a context dependent manner, whereas SIRT3 is present in mitochondria (65). As MORC2 is localized in nuclear and cytoplasm (21,26,66), we therefore focused on addressing the potential role of SIRT1 and SIRT2 in MORC2 deacetylation. Results showed that ectopic expression of SIRT2, but not SIRT1, decreased K767Ac of exogenous and endogenous MORC2 (Figure 2A and B). Moreover, expression of WT SIRT2, but not its catalytically inactive H187Y mutant (67), decreased MORC2 K767Ac (Figure 2C), indicating that the deacetylase activity of SIRT2 is required for MORC2 deacetylation. Consistently, knock-
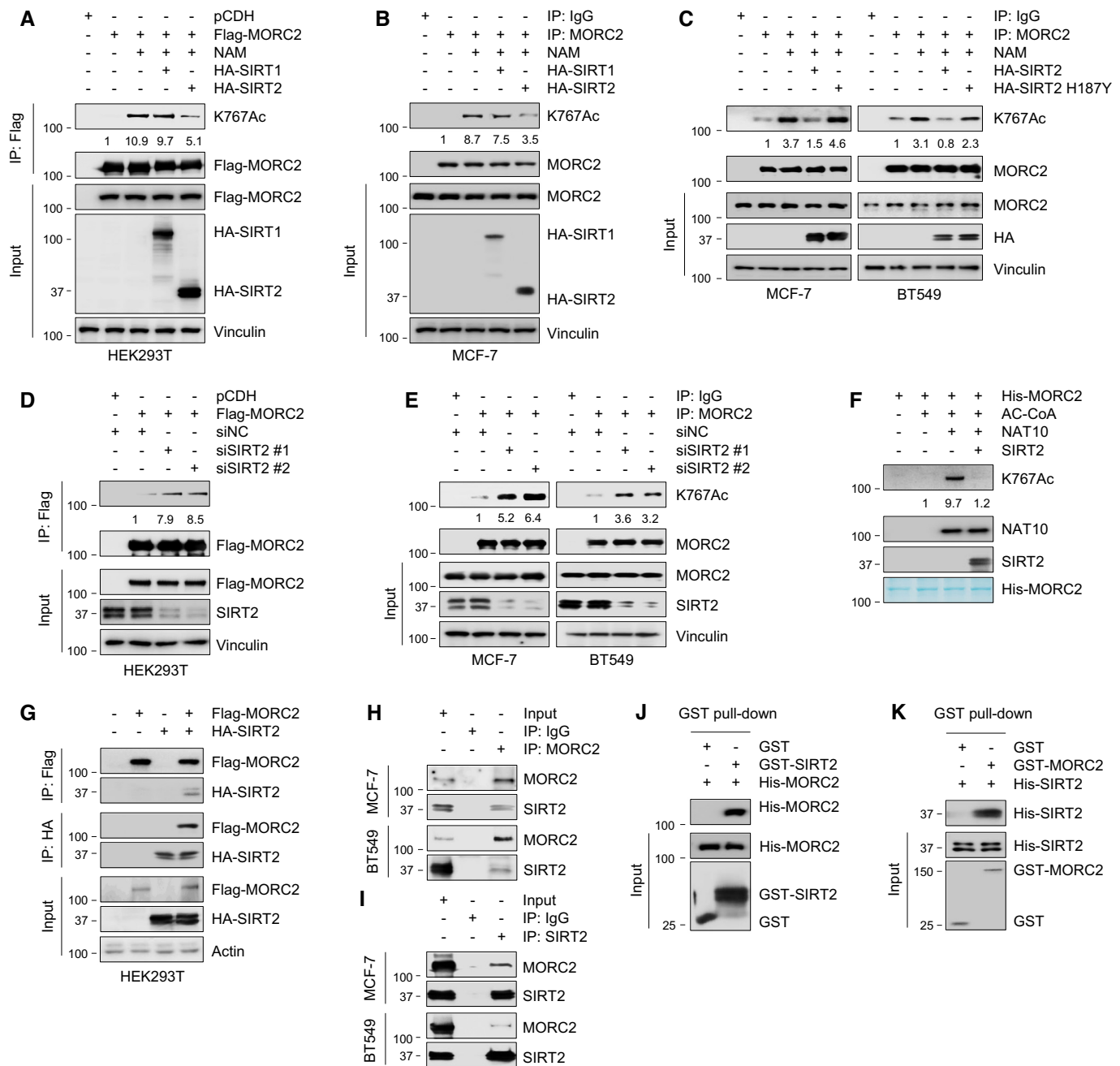
Figure 2. SIRT2 deacetylate MORC2 at K767. (**A**, **B**) HEK293T (A) and MCF-7 (B) cells were transfected with the indicated expression vectors. After 48 h of transfection, cells were treated with or without 5 mM NAM for 6 h, followed by IP and immunoblotting analysis. (**C**) MCF-7 and BT549 cells were transfected with or without expression vectors encoding HA-SIRT2 and HA-SIRT2-H187Y. After 48 h of transfection, cells were treated with or without 5 mM NAM for 6 h, followed by IP and immunoblotting analysis. (**D**, **E**) HEK293T cells stably expressing pCDH and Flag-MORC2 (D) as well as MCF-7 and BT-549 cells (E) were transfected with siNC or two siRNAs targeting SIRT2 (siSIRT2). After 48 h of transfection, lysates were subjected to IP and immunoblotting analysis. (**F**) Purified His-MORC2 was subjected to *in vitro* acetylation assays as described in Figure 1N. Then, acetylated MORC2 as a substrate was incubated with or without recombinant SIRT2 at 37°C for 2 h. The reaction mixtures were then subjected to SDS-PAGE and immunoblotted with the indicated antibodies. His-MORC2 was visualized by Coomassie blue staining. (**G**) HEK293T cells were transfected with HA-SIRT2 and Flag-MORC2 alone or in combination. IP and immunoblotting analysis was performed with the indicated antibodies after 48 h of transfection. (**H-I**) Lysates from MCF-7 and BT549 cells were subjected to IP and immunoblotting analysis with the indicated antibodies. (**J**, **K**) Reciprocal GST pull-down assays were performed using GST-SIRT2 and His-MORC2 (J) or GST-MORC2 and His-SIRT2 (K). GST was used as a negative control. Immunoblotting analysis was conducted with the indicated antibodies. GST, GST-SIRT2, or GST-MORC2 protein was visualized by Coomassie blue staining.

down of SIRT2 using two siRNAs led to an increase of K767Ac of exogenous and endogenous MORC2 (Figure 2D and E). More importantly, recombinant SIRT2 protein efficiently blocked NAT10-mediated MORC2 K767Ac *in vitro* (Figure 2F).

To unravel the mechanistic details regarding SIRT2-mediated MORC2 deacetylation, we next examined the potential interaction between SIRT2 with MORC2. As shown in Figure 2G, Flag-MORC2 co-immunoprecipitated with HA-SIRT2 when only co-expressed in HEK293T cells. Moreover, endogenous MORC2 interacted with endogenous SIRT2 in MCF-7 and BT549 cells (Figure 2H and I). Direct interaction between both proteins was further confirmed by *in vitro* GST pull-down assays (Figure 2J and K). Together, these results demonstrated that SIRT2 is the primary deacetylase for MORC2 deacetylation.

DNA-damaging agents stimulate MORC2 K767Ac in a NAT10-dependent manner

As acetylation of non-histone proteins is involved in cellular response to DNA damage (38), we next examined whether DNA-damaging agents affect MORC2 K767Ac. To do this, we treated MCF-7 and BT549 cells with or without various DNA-damaging agents, including methyl methanesulfonate (MMS), hydrogen peroxide (H_2O_2), adriamycin (ADR), cisplatin (CDDP) and ionizing radiation (IR), and then examined their effects on MORC2 K767Ac. As shown in Figure 3A, MORC2 K767Ac was upregulated by various DNA-damaging agents, and MMS and IR showed the strongest response, followed by CDDP, H_2O_2 and ADR. Consistently, K767Ac of exogenously expressed MORC2 in HEK293T cells was increased following treatment with MMS, IR and CDDP in a time- and dose-dependent manner (Supplementary Figure S3A–F, respectively). Immunofluorescent (IF) staining confirmed that treatment with MMS and IR up-regulated MORC2 K767Ac in HEK293T cells, which was effectively blocked by pre-incubation of the K767Ac antibody with the K767-acetylated peptide (Figure 3B and C). This result further demonstrated that the MORC2 K767Ac antibody is specific to recognize acetylated MORC2 at K767.

We next investigated whether NAT10 is involved in DNA damage-induced MORC2 K767Ac. Results showed that depletion of NAT10 in MCF-7 and BT549 cells using two siRNAs remarkably blocked MORC2 K767Ac upregulation induced by MMS and IR treatment (Figure 3D–F). In contrast, MMS or IR treatment still enhanced MORC2 K767Ac in SIRT2 KO cells (Figure 3G). These results suggest that NAT10, but not SIRT2, may play a major role in DNA damage-induced MORC2 K767Ac.

DNA damage enhances the interaction between NAT10 and MORC2

To gain mechanistic insights into the contribution of NAT10 to DNA damage-induced MORC2 K767Ac, we next examined whether DNA damage affect the interaction between NAT10 and MORC2. Reciprocal IP assays revealed that the interaction between MORC2 and NAT10

was enhanced following MMS and IR treatment (Figure 3H–M). Upon DNA damage, numerous proteins shuttle dynamically between the nucleolus and the nucleoplasm (68). A case in point is NAT10, which has recently been shown to translocate to the nucleoplasm from the nucleolus in response to DNA damage (43,69). IF staining showed that NAT10 was mainly localized in the nucleolus in the absence of DNA damage and co-localized with MORC2 at the edge of the nucleolus (Figure 3N). In contrast, treatment of MMS and IR resulted in a translocation of NAT10 from the nucleolus to the nucleoplasm, leading to an enhanced co-localization between NAT10 and MORC2 (Figure 3N). These results suggest that DNA damage-induced MORC2 K767Ac is likely attributable to an increase in the interaction between MORC2 and NAT10.

Acetylated MORC2 binds to H3T11P

Acetylation controls a wide variety of protein functions, such as protein stability, subcellular localization, and protein-protein interaction (38). Interestingly, cycloheximide (CHX) chase assays and immunofluorescent staining revealed that MORC2 K767Ac did not affect its half-life and subcellular localization, respectively (Figure 4A–C). Given that MORC2 is a chromatin-associated protein (18,21), we next examined whether MORC2 acetylation affects its binding with histone modification marks. To do this, we purified Flag-MORC2 K767R and Flag-MORC2 K767Q proteins from HEK293T cells and then incubated with MODified Histone Peptide Array, which contains 384 histone tail peptides carrying 59 PTMs in duplicate. According to the specificity factor, the top 10 histone modification marks with the binding activity to Flag-MORC2 K767R and Flag-MORC2 K767Q are shown in Figure 4D. Among them, H3K36Ac (acetylation of histone H3 at lysine 36) and H3T11P (phosphorylation of histone H3 at threonine 11) had the strongest binding activity to Flag-MORC2 K767R and Flag-MORC2 K767Q, respectively.

To validate the above results, we transfected pCDH or Flag-MORC2 vectors (WT, K767R, and K767Q) into HEK293T cells and performed IP assays with an anti-Flag antibody. Immunoblotting analysis showed the K767R mutant had reduced binding to H3T11P compared to WT and K767Q mutant MORC2 (Figure 4E). In addition, we noticed that WT MORC2 had lower binding activity for H3T11P than K767Q mutant did. This occurred probably due to the fact that the acetylation levels of WT MORC2 are relatively low in the absence of DNA damage. We next performed peptide pull-down assays using the unmodified or phosphorylated (T11) histone H3 peptides (amino acids 1–21) and nuclear extracts from HEK293T cells stably expressing Flag-MORC2 (WT, K767R, and K767Q). As shown in Figure 4F, WT and K767Q mutant MORC2, but not K767R mutant, bound to T11 phosphorylation-modified H3 peptide. Moreover, K767Q mutant had stronger binding ability to H3T11P peptide than WT MORC2. To test whether acetylated MORC2 directly binds to H3T11P, we purified His-MORC2 (WT and K767Q) proteins from bacteria and then subjected to pep-
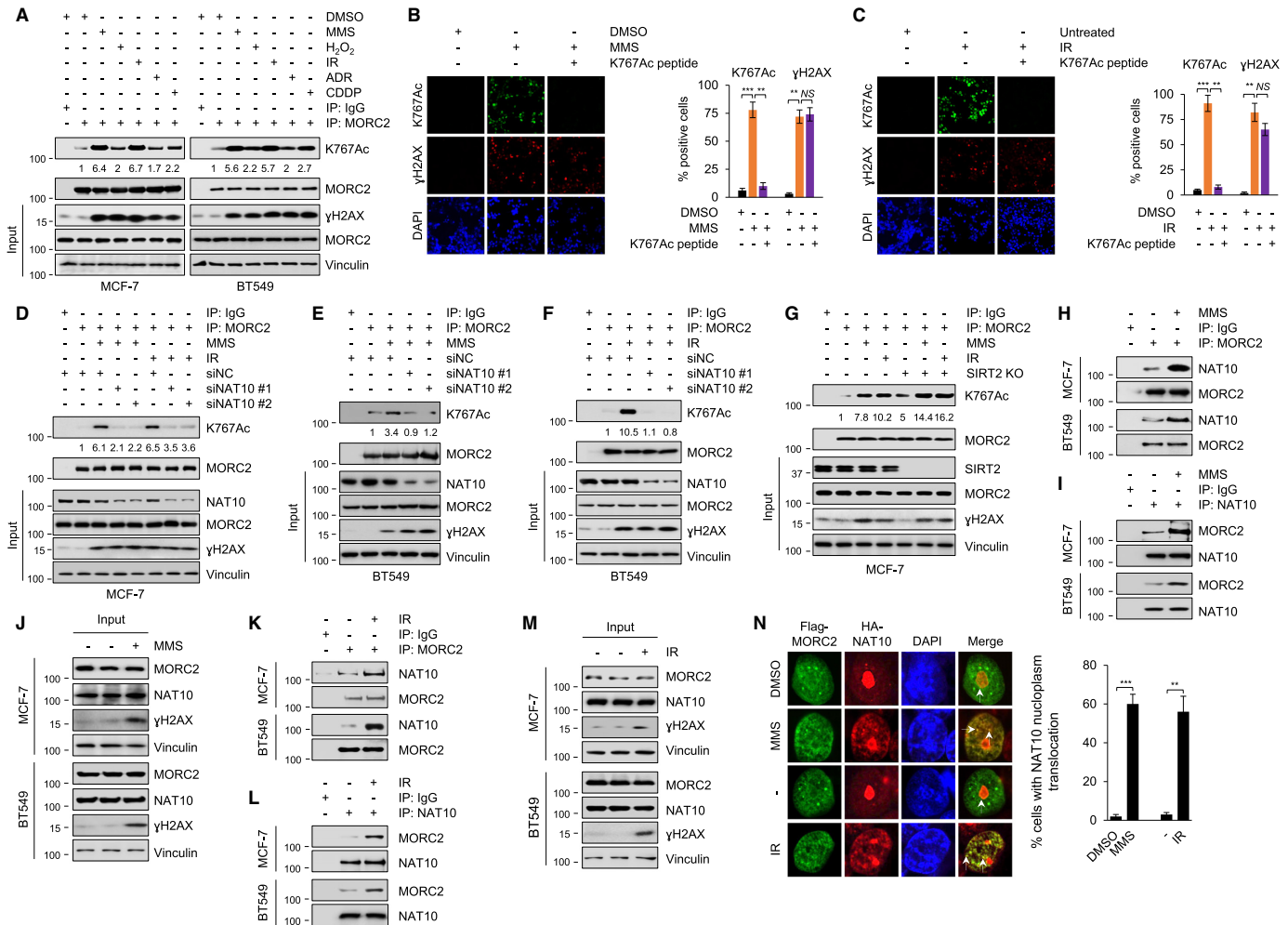
Figure 3. DNA-damaging agents stimulate MORC2 K767Ac in a NAT10-dependent manner. (**A**) MCF-7 and BT549 cells were treated with or without 1 mM MMS, 1 mM H_2O_2, 1 μM ADR, 100 μM CDDP or 6 Gy IR. After 2 h of treatment, lysates were subjected to IP and immunoblotting analyses with the indicated antibodies. MORC2 K767Ac levels were normalized to those of total MORC2 protein. (**B**, **C**) HEK293T cells were treated with or without 1mM MMS (B) or 6 Gy IR (C). After 2 h of treatment, cells were stained with MORC2 K767Ac antibody (green) and γH2AX (red). DNA was counterstained with DAPI (blue). For peptide blocking assays, K767 acetylated peptide (final concentration: 0.1 μg/μL) was added into the diluted K767Ac antibody. Quantitative results for K767Ac- and γH2AX-positively stained cells are shown in the right panel. ***, $P < 0.01$, **, $P < 0.01$. Scale bar, 25 μm. (**D**, **F**) Cells were transfected with siNC or two siNAT10s. After 48 h of transfection, cells were treated with or without 1mM MMS or 6 Gy IR for 2 h and harvested for IP and immunoblotting analysis with the indicated antibodies. (**G**) WT and SIRT2 KO MCF-7 cells were treated with or without 1 mM MMS or 6 Gy IR for 2 h and harvested for IP and immunoblotting analysis with the indicated antibodies. MORC2 K767Ac levels were normalized to those of total MORC2 protein. (**H–M**) MCF-7 and BT549 cells were treated with or without 1mM MMS or 6 Gy IR for 2 h. IP and immunoblotting analysis was conducted with the indicated antibodies. (**N**) MCF-7 cells were transfected with HA-NAT10 and Flag-MORC2. After 48 h of transfection, cells were treated with or without 1 mM MMS or 6 Gy IR for 2 h and stained with anti-Flag (green) or anti-HA (red) antibody. DNA was counterstained with DAPI (blue). Typical co-location between NAT10 and MORC2 was indicated by arrows. Quantitative results for cells with NAT10 nucleoplasm translocation are shown in the right panel. ***$P < 0.01$, **$P < 0.01$. Scale bar, 2.5 μm.

tide pull-down assays. Results showed that only K767Q mutant MORC2 could bind to T11 phosphorylation-modified H3 peptide (Figure 4G). This occurred probably due to the fact that the purified His-MORC2 WT from bacteria has no or weak acetylation modification in the absence of DNA damage. To further confirm these results, we purified His-MORC2 WT and His-MORC2 K767R and then subjected to *in vitro* acetylation assays as described in Figure 1O. Reciprocal pull-down assays demonstrated that acetylated MORC2 at K767 bound to T11 phosphorylation-modified H3 peptide (Figure 4H). Together, these results suggest that acetylated MORC2 at K767 binds to H3T11P.

MORC2 K767Ac is essential for DNA damage-induced reduction of H3T11P and transcriptional repression of its target genes *CDK1* and *Cyclin B1*

Recent reports have shown that DNA damage rapidly reduces H3T11P, and loss of H3T11P correlates with transcriptional repression of *CDK1* and *Cyclin B1* through reducing H3K9Ac at their promoters (13). We next examined whether acetylated MORC2 affects the expression levels of H3T11P and its targets *CDK1 and Cyclin B1* in response to DNA damage. Results showed that the levels of H3T11P were significantly decreased after MMS and IR treatment in WT but not MORC2 KO MCF-7 and BT549
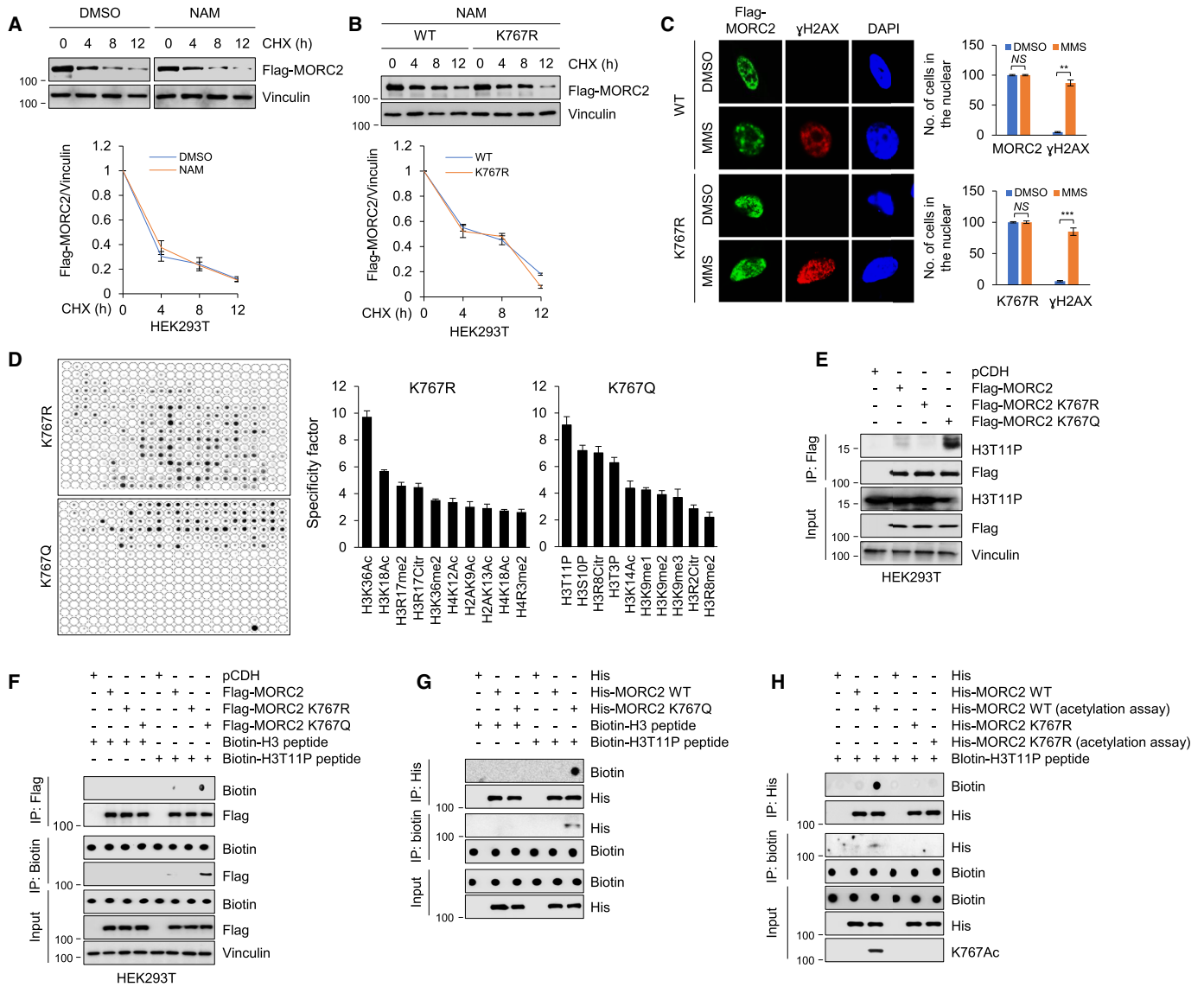
Figure 4. MORC2 K767Ac binds to H3T11P. (**A**) HEK293T cells stably expressing Flag-MORC2 were pretreated with DMSO or 5 mM NAM for 6 h and then incubated with 100 μg/ml CHX for the indicated times. Immunoblotting analysis was performed with the indicated antibodies. Relative MORC2 levels (MORC2/Vinculin) are shown in lower panels. (**B**) HEK293T cells stably expressing Flag-MORC2 or Flag-MORC2 K767R were pretreated with 5 mM NAM for 6 h and then incubated with 100 μg/ml CHX for the indicated times. Immunoblotting analysis was performed with the indicated antibodies. Relative MORC2 levels (MORC2/Vinculin) are shown in lower panels. (**C**) HEK293T cells stably expressing Flag-MORC2 or Flag-MORC2 K767R were treated with or without 1 mM MMS for 2 h and then stained with an anti-Flag (green) or an anti-γH2AX antibody. DNA was counterstained with DAPI (blue). Quantitative results for MORC2- and γH2AX-positively stained cells are shown in right panel ($n = 100$). ***$P < 0.001$, **$P < 0.01$. Scale bar, 2.5 μm. (**D**) Histone binding assays were performed using the MODified Histone Peptide Arrays (Active motif) and purified Flag-MORC2 K767R and Flag-MORC2 K767Q proteins from HEK293T cells according to the manufacturer's instructions. Signals were deleted by ECL visualization and analyzed by Array Analysis Software. The results were quantitated according to specificity factor (right panel). (**E**) HET293T cells were transfected with the indicated expression vectors. After 48 h of transfection, lysates were subjected to IP analysis with anti-Flag antibody, followed by immunoblotting analysis. (**F**) HEK293T cells were transfected with pCDH, Flag-MORC2, Flag-MORC K767R, and Flag-MORC K767Q. After 48 h of transfection, lysates were incubated with Biotin-H3 or Blotin-H3T11P peptides and then subjected to pull-down assays with Fag-beads or Streptavidin-beads, followed by immunoblotting analysis. (**G**) His, His-MORC2 WT, and His-MORC2 K767Q were purified from *E. coli* strain BL21 (DE3) and incubated with Biotin-H3 or Biotin-H3T11P peptides. The mixture was subjected to pull-down with Flag-beads or Streptavidin beads, followed by immunoblotting analysis. (**H**) His-MORC2 WT and His-MORC2 K767R were pre-incubated with NAT10 in HAT buffer to be acetylated and then incubated with Biotin-H3 or Biotin-H3T11P peptides, followed by pull-down and immunoblotting analysis.
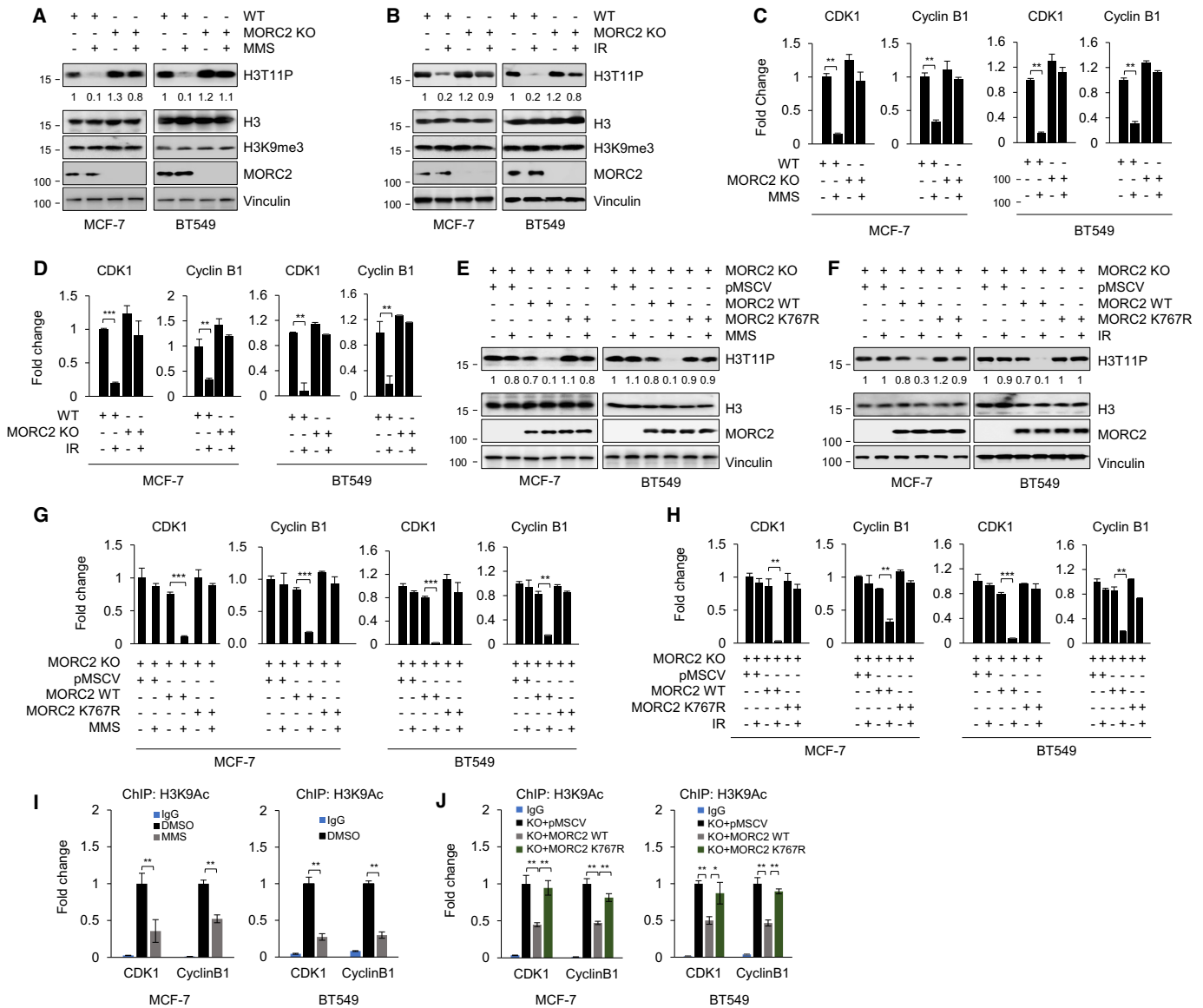
Figure 5. MORC2 K767Ac is required for DNA damage-induced downregulation of H3T11P and transcriptional repression of *CDK1* and *Cyclin B1*. (**A–D**) WT and MORC2 KO MCF-7 and BT549 cells were treated with or without 1 mM MMS or 6 Gy IR for 2 h and subjected to immunoblotting with the indicated antibodies (A and B) or qPCR analysis of *CDK1* and *CyclinB1* mRNA levels (C and D). (**E–H**) MORC2 KO MCF-7 and BT549 cells were transfected with plasmid DNAs encoding pMSCV, Flag-MORC2 or Flag-MORC2 K767R. After 48 h of transfection, cells were treated with or without 1 mM MMS or 6 Gy IR for 2 h and subjected to immunoblotting (E and F) and qPCR analysis (G and H). (**I**) MCF-7 and BT549 cells were treated with or without 1 mM MMS for 2 h and subjected to ChIP assays with an anti-H3K9Ac antibody, followed by qPCR analysis. Recruitment of H3K9Ac to *CDK1* and *Cyclin B1* promoter was normalized to the Input. (**J**) MORC2 KO MCF-7 and BT549 cells expressing pMSCV, MORC2 WT, and MORC2 K767R were treated with or without 1 mM MMS for 2 h and subjected to ChIP-qPCR analysis as described in I.

cells (Figure 5A and B). In addition, protein and mRNA levels of CDK1 and CyclinB1 were reduced following MMS and IR treatment in WT but not MORC2 KO MCF-7 and BT549 cells (Figure 5C and D, and Supplementary Figure S4A and B). These results suggest that MORC2 mediates DNA damage-induced reduction of H3T11P, CDK1, and Cyclin B1.

To test whether MORC2 K767Ac contributes to regulation of H3T11P, we infected MORC2 KO MCF-7 and BT549 cells with lentiviral expression vectors encoding empty vector pMSCV, Flag-MORC2, Flag-MORC2 K767R and then treated with or without MMS and IR. Im-

munoblotting analysis revealed that treatment with MMS and IR led to a decrease in H3T11P in WT MORC2 expressing cells but not in cells expressing pMSCV and K767R mutant MORC2 (Figure 5E and F). The similar trend was also observed for *CDK1* and *Cyclin B1* protein and mRNA levels (Figure 5G and H, and Supplementary Figure S4C and S4D). ChIP assays demonstrated that treatment with MMS and IR reduced the presence of H3K9Ac at the promoters of *CDK1* and *Cyclin B1* (Figure 5I). Moreover, H3K9Ac levels at *CDK1* and *Cyclin B1* promoters were significantly lower in WT MORC2 expressing cells than cells expressing pMSCV and K767R MORC2 after
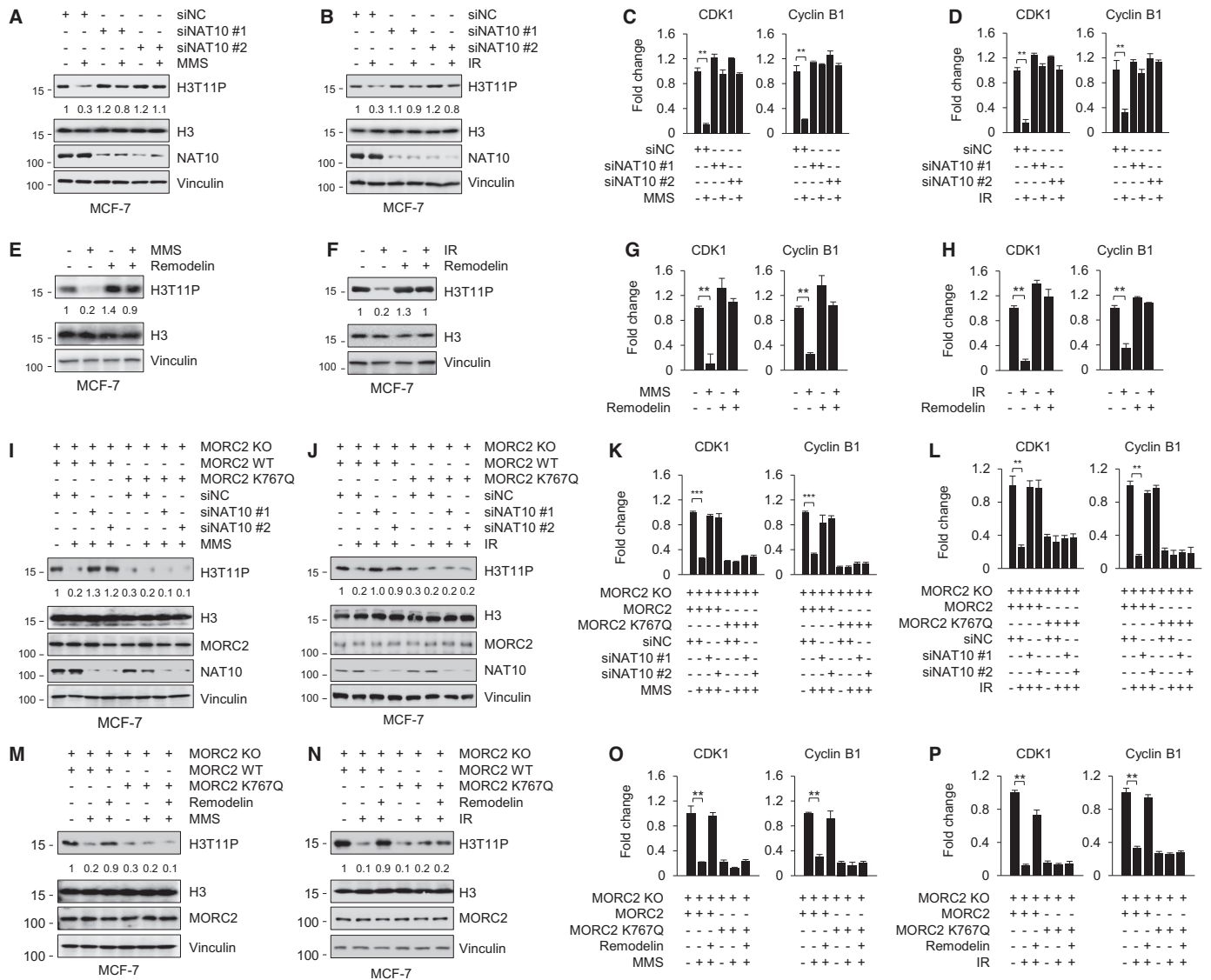
Figure 6. NAT10 regulates H3T11P, CDK1, and Cyclin B1 expression through MORC2 K767Ac. (**A–D**) MCF-7 cells were transfected with siNC or two siNAT10s. After 48 h of transfection, cells were treated with or without 1 mM MMS or 6 Gy IR for 2 h and then subjected to immunoblotting (A-B) and qPCR analysis (C-D). (**E–H**) MCF-7 cells were pretreated with or without 5 μM Remodelin for 3 h, followed by treatment with or without 1 mM MMS or 6 Gy IR for another 2 h. Immunoblotting (E, F) and qPCR analyses (G-H) were performed as indicated. (**I–L**) MORC2 KO MCF-7 cells stably expressing Flag-MORC2 and Flag-MORC2 K767Q were transfected with siNC or two siNAT10s. After 48 h of transfection, cells were treated with or without 1mM MMS or 6 Gy IR for 2 h and then subjected to immunoblotting (I and J) and qPCR analysis (K and L). (**M–P**) MORC2 KO MCF-7 cells expressing Flag-MORC2 and Flag-MORC2 K767Q were pretreated with or without 5 μM Remodelin for 3 h, followed by treatment with or without 1 mM MMS or 6 Gy IR for another 2 h. Immunoblotting (M and N) and qPCR analyses (O and P) were performed as indicated.

MMS treatment (Figure 5J). Together, these results suggest that MORC2 K767Ac contributes to DNA damage-induced loss of H3T11P and transcriptional repression of *CDK1* and *Cyclin B1*.

Recent studies have shown that DNA damage rapidly reduces H3T11P through activating protein phosphatase 1γ (PP1γ) (12) or releasing CHK1 kinase from chromatin (13). To address how MORC2 K767Ac regulates H3T11P, we first examined whether MORC2 affects the levels of phosphorylated CHK1 at serine 345 (p-CHK1 S345) and phosphorylated CHK2 at threonine 68 (p-CHK2 T68). Results showed that knockout of MORC2 in both MCF-7 and BT549 cells did not significantly affect MMS- and

IR-induced increase in the levels of p-CHK1 S345 and p-CHK2 T68 (Supplementary Figure S4A and B). Moreover, treatment with MMS and IR led to a similar increase in the levels of p-CHK1 S435 and p-CHK2 T68 in MORC2 KO BT549 cells reexpressing pMSCV, WT MORC2, and K767R mutant MORC2 (Supplementary Figure S4C and S4D). These results suggest that MORC2 does not affect CHK1 and CHK2 activation in response to DNA damage. Then, we carried out IP assays to examine whether DNA damage affects the interaction between MORC2 and PP1γ. Results showed that treatment of MCF-7 cells with IR resulted in an increase in the interaction between MORC2 and PP1γ (Supplementary Figure
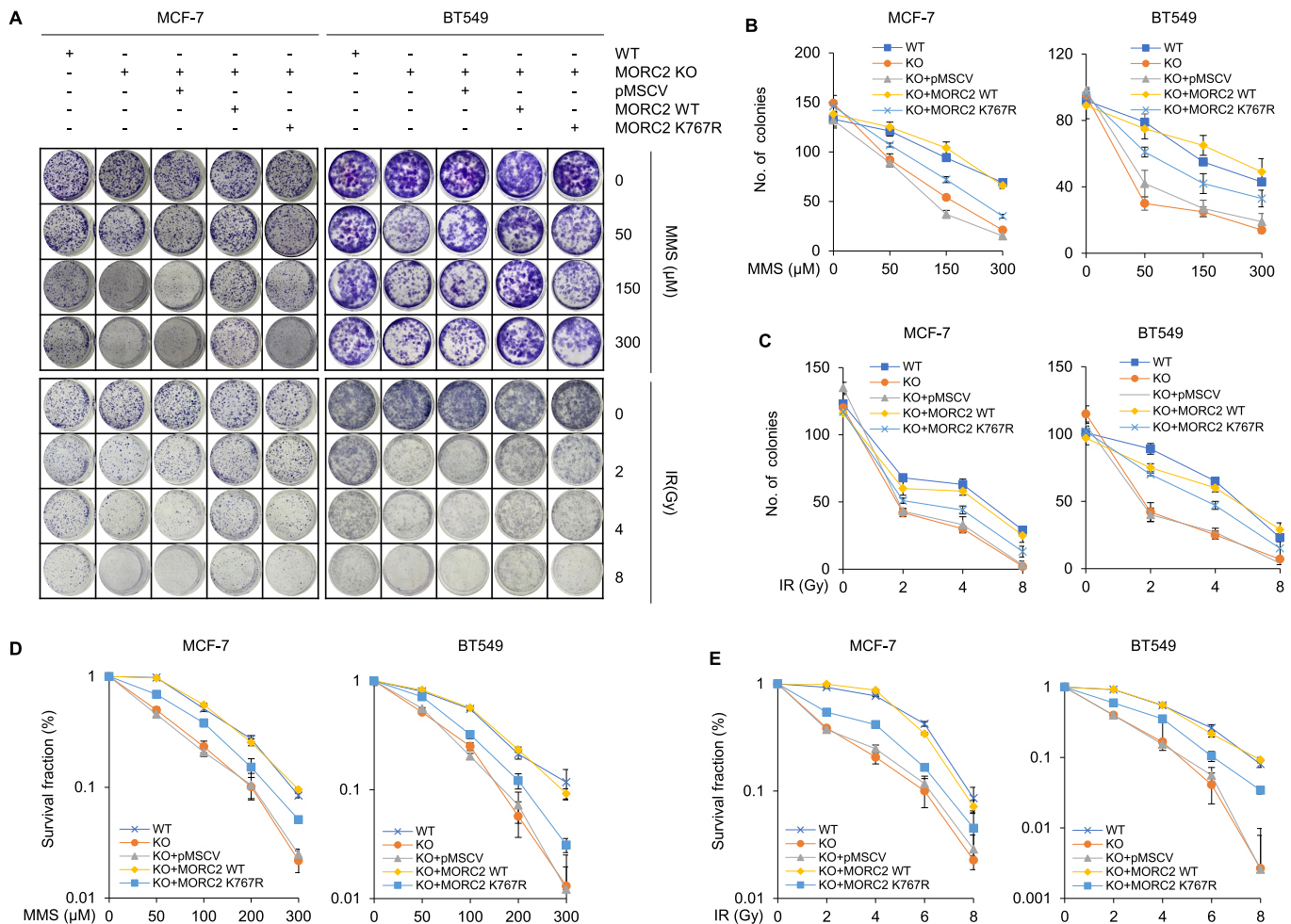
Figure 7. MORC2 K767Ac is essential for cell survival in response to MMS and IR treatment. (**A–C**) MORC2 KO MCF-7 and BT549 cells stably expressing pMSCV, Flag-MORC2 or Flag-MORC2 K767R were treated with increasing doses of MMS or IR and subjected to colony formation survival assays. Representative images of survival colonies are shown in A and corresponding quantitative results are shown B and C. (**D** and **E**) MORC2 KO MCF-7 and BT549 cells stably expressing pMSCV, MORC2 and MORC2 K767R were treated with increasing doses of MMS (D) or IR (E) for 48 h and subjected to CCK-8 assays.

S4E–G), but MORC2 K767Ac did not affect the noted interaction between MORC2 and PP1γ (Supplementary Figure S4H). Given that MORC2 K767Ac affected the interaction between MORC2 and H3T11P (Figure 4), we speculate that MORC2 affects H3T11P dephosphorylation following DNA damage through, at least in part, recruiting PP1γ to chromatin.

NAT10 regulates H3T11P, CDK1, and Cyclin B1 expression through MORC2 K767Ac

As NAT10 regulates MORC2 K767Ac, we next examined whether NAT10 affects H3T11P, CDK1, and Cyclin B1 expression in response to DNA damage. As expected, knockdown of NAT10 by two siRNAs compromised MMS- and IR-induced downregulation of H3T11P (Figure 6A and B) and transcriptional repression of *CDK1* and *Cyclin B1* (Figure 6C and D). Similarly, IR- and MMS-induced H3T11 dephosphorylation and transcription repression of *CDK1* and *Cyclin B1* were compromised in the presence of NAT10 in-

hibitor Remodelin (Figure 6E–H). Moreover, knockdown of NAT10 (Figure 6I–L) or chemical inhibition of NAT10 by Remodelin (Figure 6M–P) compromised MMS- and IR-induced H3T11 dephosphorylation and transcriptional repression of *CDK1* and *Cyclin B1* in cells expressing WT MORC2 but not K767Q mutant MORC2. These results suggest that NAT10 regulates DNA damage-induced H3T11 dephosphorylation and transcription repression of *CDK1* and *Cyclin B1* through MORC2 K767Ac.

Acetylated MORC2 is required for the G2 checkpoint arrest and confers resistance to MMS and IR

CDK1 and Cyclin B1 are key regulators for transition though the G2 phase and entry into mitosis during normal cell cycle. Transcriptional repression of *CDK1* and *Cyclin B1* or inactivation of CDK1 and Cyclin B1 activity during DNA damage induces G2/M cell cycle arrest (13,70). To examine the role of MORC2 acetylation in cell cycle checkpoint activation, we reconstituted empty vector pMSCV,
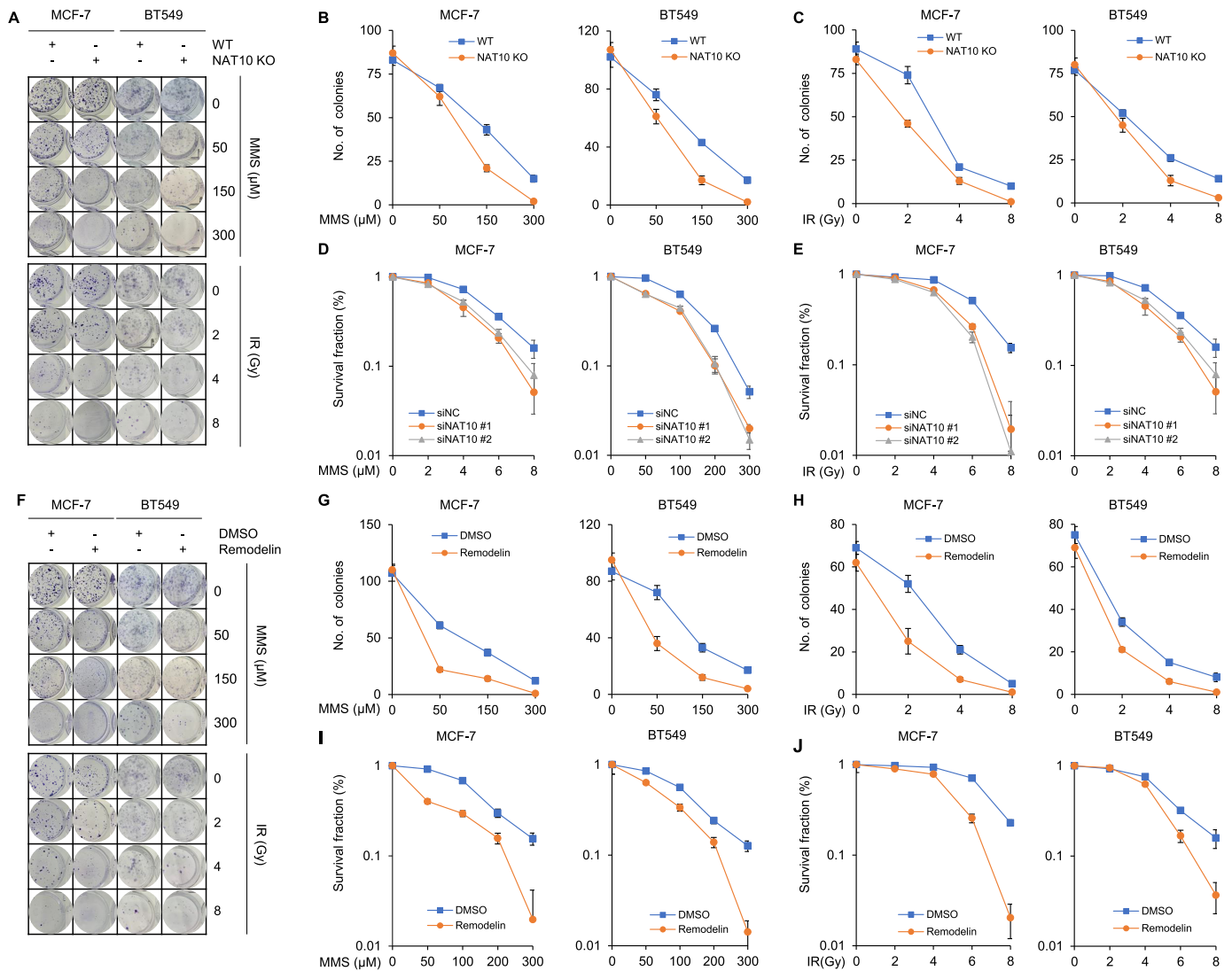
Figure 8. NAT10 is essential for cell survival in response to MMS and IR treatment. (**A–C**) WT and NAT10 KO MCF-7 and BT549 stable cells were treated with or without increasing doses of MMS or IR and subjected to colony formation survival assays. Representative images of survival colonies are shown A, and corresponding quantitative results are shown B and C. (**D** and **E**) MCF-7 and BT549 cells were transfected with siNC or two siNAT10s. After 24 h of transfection, cells were treated with increasing doses of MMS (D) or IR (E). After 48 h of treatment, cells were subjected to CCK-8 assays. (**F–H**) MCF-7 and BT549 cells were treated with increasing doses of MMS or IR and subjected to colony formation survival assays. DMSO or 5 μM Remodelin was added to culture medium. Representative images of survival colonies are shown in F, and corresponding quantitative results of survival colonies are shown in G and H. (**I** and **J**) MCF-7 and BT549 cells were treated with increasing doses of MMS or IR. After 48 h of treatment, cells were subjected to CCK-8 assays. DMSO or 5 μM Remodelin was added to culture medium.

WT or K767R mutant MORC2 into MORC2 KO MCF-7 and BT549 (Supplementary Figure S5A). Then, we treated the established cells with or without IR. Analysis of the cell-cycle distribution using fluorescence-activated cell sorting (FACS) showed that treatment of control cells with IR resulted in a remarkable arrest at the G2/M phase in WT cells, which was diminished in MORC2 KO cells (Supplementary Figure S5B and C). Moreover, reintroduction of WT MORC2, but not K767R mutant, in MORC2 KO cells restored IR-induced G2/M arrest (Supplementary Figure S5B and C). These results suggest that MORC2 K767Ac contributes to IR-induced G2/M checkpoint activation. As MORC2 KO cells failed to accumulate in G2/M after DNA damage, we next investigated whether they remained ar-

rested in the G1/S phase or overrode the checkpoint to accumulate in next G1/S phase. Toward this aim, WT cells and MORC2 KO MCF-7 and BT549 cells stably expressing pMSCV, Flag-MORC2, or Flag-MORC2 K767R were treated with or without 10 Gy IR alone or in combination with 500 ng/ml nocodazole, a widely used cell cycle synchronizing agent to induce mitotic arrest. FACS analysis showed that MORC2 KO cells were arrested in M phase in the presence of nocodazole, indicating that MORC2 mainly affects G2/M checkpoint arrest (Supplementary Figure S6A and B). To distinguish the impact of MORC2 on the G2 or M phase of cell cycle, we carried out FACS analysis using an anti-mitotic protein antibody [MPM-2] to detect mitotic cells. The MPM-2 antibody recognizes a
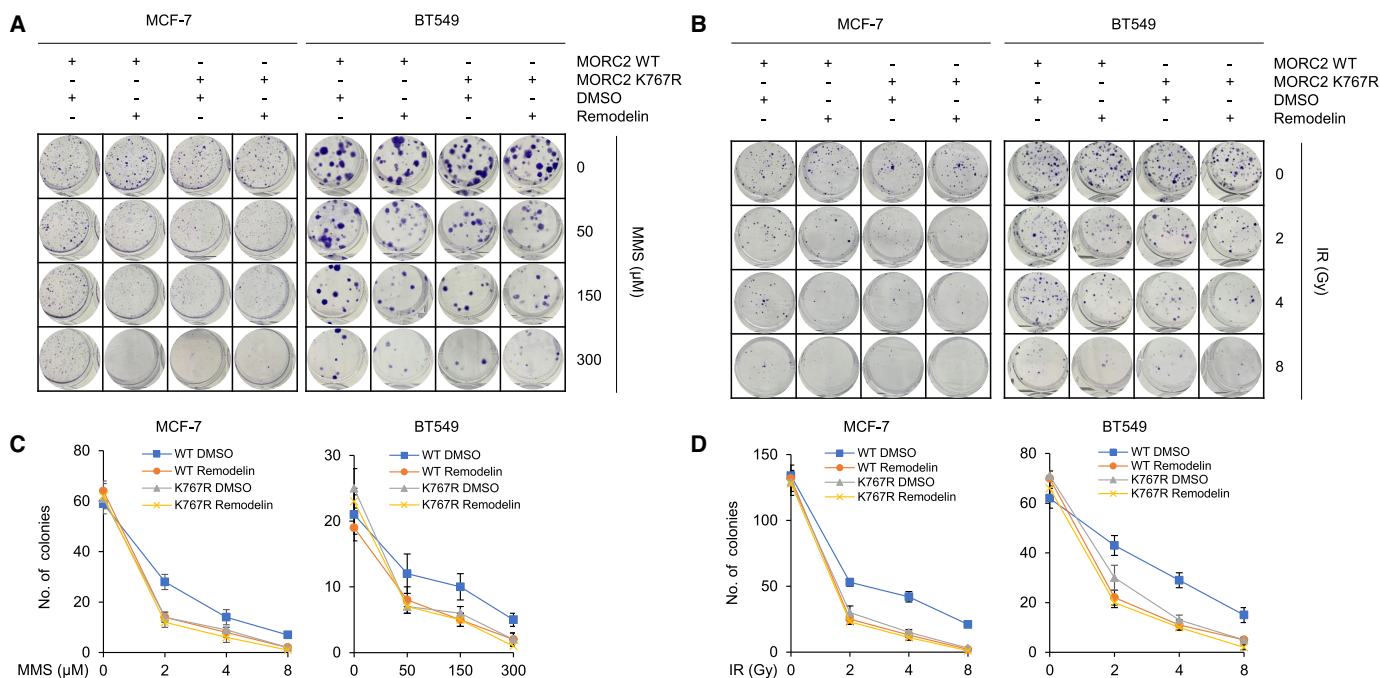
Figure 9. NAT10 inhibitor Remodelin enhances the sensitivity of cells expressing WT MORC2, but not K767R mutant MORC2, to MMS and IR. (**A–D**) MORC2 KO MCF-7 and BT549 cells stably expressing Flag-MORC2 or Flag-MORC2 K767R were treated with increasing doses of MMS (A) or IR (B) and subjected to colony formation survival assays. DMSO or 5 μM Remodelin was added to culture medium. Representative images of survival colonies are shown in A and B, and corresponding quantitative results are shown in C and D.

group of phosphorylated forms of proteins that are phosphorylated only in mitosis (71). Results showed that the percentage of MPM-2 positive cells was significantly decreased after IR treatment in WT MCF-7 and BT549 cells and MORC2 KO cells re-expressing WT MORC2, as compared with MORC2 KO cells expressing empty vector or K767R mutant MORC2 (supplementary Figure S7A and B). In support of our results, previous studies have demonstrated that radiation-induced cell cycle arrest is specific to G2 phase (72) and that the mitotic population of cancer cells is significantly decreased following IR treatment (72–74). Together, these results suggest that MORC2 K767Ac is required for G2 checkpoint arrest in response to genotoxic stress, thus blocking cells to progress through mitosis. Without functional G2 blockade, damaged cells may not be able to repair DNA damage before entering mitosis, leading to mitotic catastrophe (75). Immunofluorescant staining showed that MORC2 KO cells and K767R mutant MORC2 expressing KO cells had more fragmented nuclei after IR treatment than WT cells and MORC2 KO cells re-expressing WT MORC2 (Supplementary Figure S8A and B).

As checkpoints are critical for cell survival by limiting cell-cycle progression following DNA damage, we next analyzed the effects of MORC2 acetylation on the sensitivity of MCF-7 and BT549 cells to MMS and IR. Colony formation survival assays showed that depletion of MORC2 resulted in enhanced cellular sensitivity to MMS and IR, which was rescued by reintroduction of WT MORC2, but not K767R mutant MORC2, into MORC2-depleted cells (Figure 7A–C). Similar results were obtained from CCK-8 assays (Figure 7D and E).

Then, we knocked out NAT10 in MCF-7 and BT549 cells and treated with or without MMS and IR. Colony survival assays showed that NAT10 KO cells were more sensitive to MMS and IR (Figure 8A–C). CCK-8 assays also demonstrated that knockdown of NAT10 in MCF-7 and BT549 cells by two siRNAs resulted in enhanced sensitivity to MMS and IR (Figure 8D and E). The similar results were obtained by chemical inhibitor of NAT10 using Remodelin (Figure 8F–J). Moreover, treatment with NAT10 inhibitor Remodelin enhanced the sensitivity of cells expressing WT MORC2, but not K767R mutant MORC2, to MMS and IR (Figure 9A–D). Collectively, these results suggest that MORC2 K767Ac is required for the G2 checkpoint activation and confers resistance to MMS and IR.

MORC2 K767Ac positively correlates with NAT10 expression in human breast tumor samples

To examine the clinical relevance of our findings, we first evaluated the expression levels of NAT10, MORC2 K767Ac, and MORC2 in 16 pairs of primary breast tumor specimens and matched adjacent noncancerous breast tissues by immunoblotting (Figure 10A). Quantitative and statistical analysis showed that the expression levels of MORC2 K767Ac and NAT10 were upregulated in breast tumor specimens as compared with the corresponding normal tissues (Figure 10B and C) and that there was a positive correction in expression levels between NAT10 and MORC2 K767Ac in those samples (Figure 10D, $P =$ 0.0445).

To verify these results, we collected 128 surgical specimens from patients diagnosed with invasive breast can-
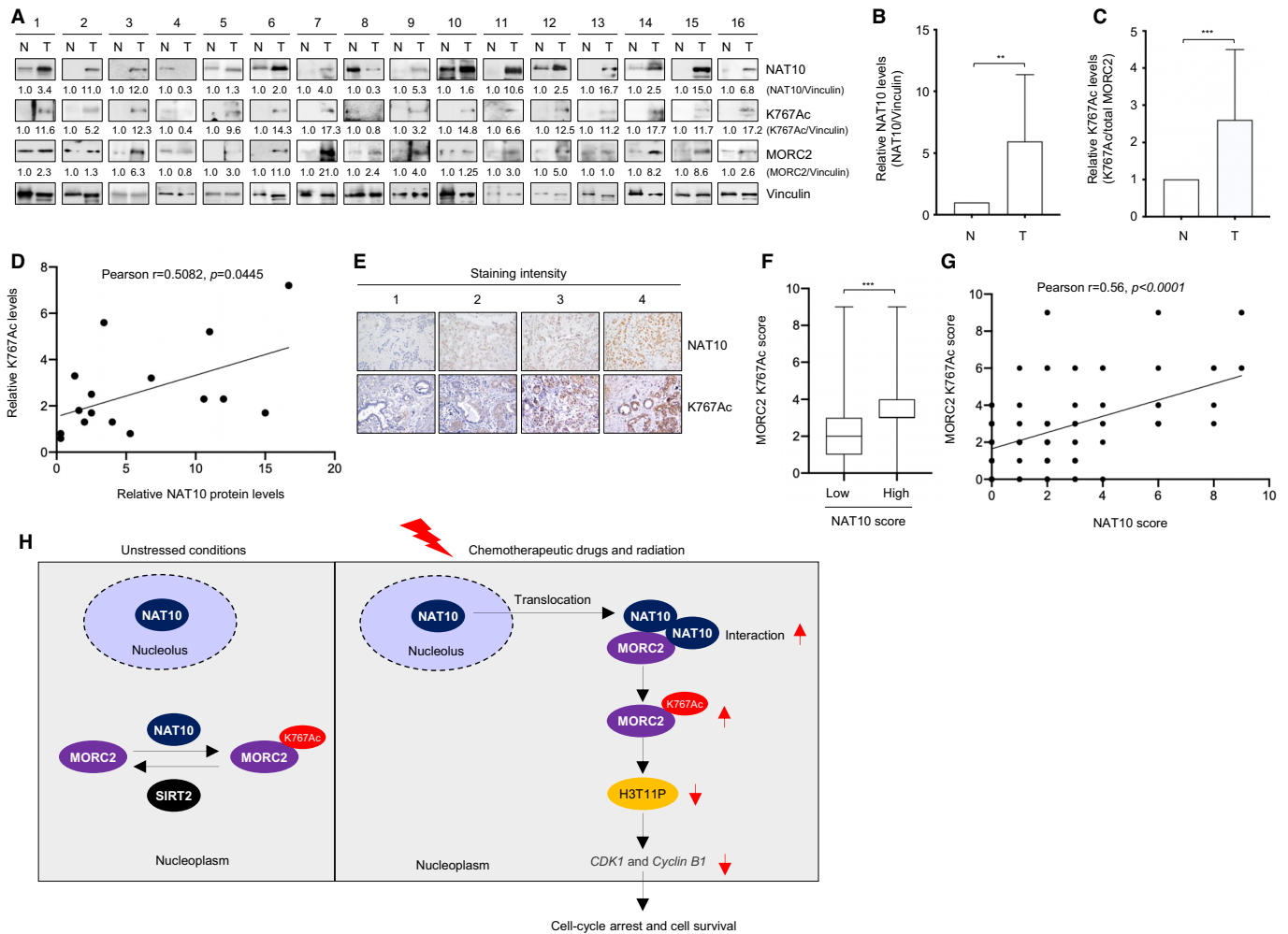
Figure 10. MORC2 K767 is positively associated with NAT10 expression levels in clinical breast tumor samples. (**A**) Lysates from 16 pairs of human breast tumor tissues (T) and adjacent noncancerous normal tissues (N) were subjected to immunoblotting analysis with the indicated antibodies. The expression levels of NAT10, MORC2, and MORC2 K767Ac were normalized to those of Vinculin. (**B**, **C**) Relative expression levels of NAT10 (**B**) and MORC2 K767Ac (**C**) in normal breast and breast tumor tissues. The expression levels of MORC2 K767Ac were normalized to those of total MORC2. (**D**) Correlation analysis of expression levels between NAT10 and MORC2 K767Ac. (**E**) IHC staining of NAT10 and MORC2 K767Ac in 128 human breast tumor specimens. Representative images are shown. Scale bars, 50 μm. (**F**) The staining score of MORC2 K767Ac in breast tumor samples correlates with that of NAT10. ***$P < 0.001$. (**G**) Correction analysis of NAT10 and MORC2 K767Ac expression levels in 128 breast tumor tissues. Pearson correlation test was used. (**H**) The proposed working model. Under unstressed conditions, MORC2 is acetylated by NAT10 and deacetylated by SIRT2 at K767. DNA damage induced by chemotherapeutic drugs and ionizing radation promotes the translocation of NAT10 from the nucleous to the nucleoplasm, resulting in enhanced interaction between MORC2 and NAT10 and subsequent MORC2 K767Ac. MORC2 K767Ac mediates DNA damage-induced reduction of H3T11P and transcriptional repression of its downstream target genes *CDK1* and *Cyclin B1*, thus contributing to DNA damage-induced G2 checkpoint activation and facilitating cell survival.

cer and determined the expression status of NAT10 and MORC2 K767Ac in these samples by immunohistochemical (IHC) staining. Validation of the NAT10 (Abcam, ab194297) antibody for IHC staining is available on-line from the manufacturers. We found that anti-MORC2 K767Ac antibody could detect strong signals in paraffin-embedded breast cancer tissues that were specifically blocked by the acetyl-K767 antigen peptide (Supplementary Figure S9), demonstrating that this antibody is suitable for IHC staining. Representative IHC images are shown in Figure 10E. According to the median staining score, these samples were divided into high and low expression groups. Of the 128 patients studied, 42.9% (55/128) and 51.6% (66/128) of patients had high NAT10 and MORC2 K767Ac

expression, respectively. As expected, a positive correlation between the levels of NAT10 and MORC2 K767Ac was observed in these samples (Figure 10F and G, $P < 0.001$). Together, these results suggest a positive correlation exists between NAT10 and MORC2 K767Ac in breast cancer samples.

DISCUSSION

Identification of signaling pathways governing DDR is important not only for gaining mechanistic insights into tumorigenesis, but also for development of novel cancer therapy strategies. In this study, we uncovered several interesting findings concerning the regulation and functions

of NAT10-mediated MORC2 acetylation in DNA damage checkpoint activation and resistance to DNA-damaging therapeutic agents in breast cancer cells (Figure 10H).

First, we identify lysine acetylation as a novel PTM of MORC2, which is oppositely regulated by the acetyltransferase NAT10 and the deacetylase SIRT2. Emerging evidence shows that MORC2 is a key player in tumorigenesis and tumor progression (26,31–35) and that mutations in MORC2 are present in hereditary Charcot-Marie-Tooth disease (18,22–25) and in cancer patients (26,76), highlighting the emerging importance of MORC2 in human diseases. However, how MORC2 is regulated still remains a gross mystery. In this study, we showed that MORC2 is an acetylated protein and is a novel substrate of NAT10 (Figure 1 and Supplementary Figure S1). Furthermore, a positive correlation between NAT10 and MORC2 K767Ac levels was observed in clinical breast tumor samples (Figure 10). SIRT2 was originally identified as a cytoplasmic KDAC responsible for α-tubulin acetylation (67). Subsequent studies revealed that it can shuttle to the nucleus to target nuclear proteins for acetylation, such as p300 (77) and histone H3 (78). We demonstrated that ectopic overexpression of SIRT2, but not its catalytically inactive mutant, decreased MORC2 K767Ac. Conversely, treatment with SIRT inhibitor NAM or depletion of SIRT2 increased MORC2 K767Ac (Figure 2). These results establish SIRT2 as a deacetylase for MORC2 deacetylation.

Second, DNA-damaging agents stimulate MORC2 K767Ac in a NAT10 dependent manner. Execution of the DDR relies upon dynamic protein modifications, such as phosphorylation, PARylation, and acetylation, which have taken center stage as important DDR regulators (64,79). In this study, we demonstrated that DNA-damaging chemotherapeutic agents and IR stimulate MORC2 K767Ac, and this process depends on NAT10. In addition, we recently demonstrated that MORC2 is modified by phosphorylation and poly(ADP-ribosyl)ation in response to DNA damage (21,36). Thus, whether there is a crosstalk among these PTMs of MORC2 during DDR remains to be addressed in the near future.

Third, acetylated MORC2 is required for the activation of the G2 checkpoint, thus contributing to enhanced cell survival following DNA damage. Recent studies have shown that DNA damage rapidly reduces H3T11P, and DNA damage-induced dephosphorylation of H3T11P contributes to subsequent transcriptional repression of *CDK1* and *Cyclin B1* (13). In this study, we discovered that MORC2 K767Ac binds to H3T11P and is required for DNA damage-induced reduction of H3T11P and transcriptional repression of *CDK1* and *Cyclin B1* (Figures 4–6). Consequently, acetylated MORC2 contributes to G2 DNA damage checkpoint activation (Supplementary S5-S7). Furthermore, chemical inhibition or depletion of NAT10 or expression of an acetylation-deficient mutant MORC2 sensitizes breast cancer cells to MMS and IR (Figures 7–9). In agreement with our findings, NAT10 has recently been shown to promote resistance to doxorubicin in liver and breast cancer cells by regulating the epithelial-mesenchymal transition (80,81). Thus, we provide new mechanism by which NAT10 contributes to resistance to MMS and IR through regulating MORC2 acetylation and G2 DNA damage checkpoint activation. Together, these results suggest that MORC2 K767Ac can function as a mediator for DDR signals to activate the G2 checkpoint, thus maintaining genome integrity and facilitating cell survival after exposure to DNA-damaging agents.

In summary, findings presented here uncover a previously unrecognized function and regulatory mechanism for MORC2 by lysine acetylation in regulating cell-cycle progression and resistance to DNA-damaging chemotherapy and radiotherapy in breast cancer cells (Figure 10H). As the NAT10 chemical inhibitor Remodelin has been characterized (47,48), it is conceivable that Remodelin might be a promising drug for sensitizing breast cancer cells to DNA-damaging chemotherapy and radiotherapy.

SUPPLEMENTARY DATA

Supplementary Data are available at NAR Online.

REFERENCES

1. Curtin,N.J. (2012) DNA repair dysregulation from cancer driver to therapeutic target. *Nat. Rev. Cancer*, **12**, 801–817.
2. Bouwman,P. and Jonkers,J. (2012) The effects of deregulated DNA damage signalling on cancer chemotherapy response and resistance. *Nat. Rev. Cancer*, **12**, 587–598.
3. Branzei,D. and Foiani,M. (2008) Regulation of DNA repair throughout the cell cycle. *Nat. Rev. Mol. Cell Biol.*, **9**, 297–308.
4. Sancar,A., Lindsey-Boltz,L.A., Unsal-Kacmaz,K. and Linn,S. (2004) Molecular mechanisms of mammalian DNA repair and the DNA damage checkpoints. *Annu. Rev. Biochem.*, **73**, 39–85.
5. Sabapathy,K. and Lane,D.P. (2018) Therapeutic targeting of p53: all mutants are equal, but some mutants are more equal than others. *Nat. Rev. Clin. Oncol.*, **15**, 13–30.
6. Bykov,V.J.N., Eriksson,S.E., Bianchi,J. and Wiman,K.G. (2018) Targeting mutant p53 for efficient cancer therapy. *Nat. Rev. Cancer*, **18**, 89–102.
7. Ashwell,S. and Zabludoff,S. (2008) DNA damage detection and repair pathways–recent advances with inhibitors of checkpoint kinases in cancer therapy. *Clin. Cancer Res.*, **14**, 4032–4037.
8. Saldivar,J.C., Cortez,D. and Cimprich,K.A. (2017) The essential kinase ATR: ensuring faithful duplication of a challenging genome. *Nat. Rev. Mol. Cell Biol.*, **18**, 622–636.

9. Castedo,M., Perfettini,J.L., Roumier,T., Andreau,K., Medema,R. and Kroemer,G. (2004) Cell death by mitotic catastrophe: a molecular definition. *Oncogene*, **23**, 2825–2837.

10. Lobrich,M. and Jeggo,P.A. (2007) The impact of a negligent G2/M checkpoint on genomic instability and cancer induction. *Nat. Rev. Cancer*, **7**, 861–869.

11. Metzger,E., Yin,N., Wissmann,M., Kunowska,N., Fischer,K., Friedrichs,N., Patnaik,D., Higgins,J.M., Potier,N., Scheidtmann,K.H. *et al.* (2008) Phosphorylation of histone H3 at threonine 11 establishes a novel chromatin mark for transcriptional regulation. *Nat. Cell Biol.*, **10**, 53–60.

12. Shimada,M., Haruta,M., Niida,H., Sawamoto,K. and Nakanishi,M. (2010) Protein phosphatase 1gamma is responsible for dephosphorylation of histone H3 at Thr 11 after DNA damage. *EMBO Rep.*, **11**, 883–889.

13. Shimada,M., Niida,H., Zineldeen,D.H., Tagami,H., Tanaka,M., Saito,H. and Nakanishi,M. (2008) Chk1 is a histone H3 threonine 11 kinase that regulates DNA damage-induced transcriptional repression. *Cell*, **132**, 221–232.

14. Narlikar,G.J., Sundaramoorthy,R. and Owen-Hughes,T. (2013) Mechanisms and functions of ATP-dependent chromatin-remodeling enzymes. *Cell*, **154**, 490–503.

15. Iyer,L.M., Abhiman,S. and Aravind,L. (2008) MutL homologs in restriction-modification systems and the origin of eukaryotic MORC ATPases. *Biol. Direct*, **3**, 8.

16. Li,D.Q., Nair,S.S. and Kumar,R. (2013) The MORC family: new epigenetic regulators of transcription and DNA damage response. *Epigenetics*, **8**, 685–693.

17. Dong,W., Vannozzi,A., Chen,F., Hu,Y., Chen,Z. and Zhang,L. (2018) MORC domain definition and evolutionary analysis of the MORC gene family in green plants. *Genome Biol. Evol.*, **10**, 1730–1744.

18. Tchasovnikarova,I.A., Timms,R.T., Douse,C.H., Roberts,R.C., Dougan,G., Kingston,R.E., Modis,Y. and Lehner,P.J. (2017) Hyperactivation of HUSH complex function by Charcot-Marie-Tooth disease mutation in MORC2. *Nat. Genet.*, **49**, 1035–1044.

19. Douse,C.H., Bloor,S., Liu,Y., Shamin,M., Tchasovnikarova,I.A., Timms,R.T., Lehner,P.J. and Modis,Y. (2018) Neuropathic MORC2 mutations perturb GHKL ATPase dimerization dynamics and epigenetic silencing by multiple structural mechanisms. *Nat. Commun.*, **9**, 651.

20. Dutta,R. and Inouye,M. (2000) GHKL, an emergent ATPase/kinase superfamily. *Trends Biochem. Sci.*, **25**, 24–28.

21. Li,D.Q., Nair,S.S., Ohshiro,K., Kumar,A., Nair,V.S., Pakala,S.B., Reddy,S.D., Gajula,R.P., Eswaran,J., Aravind,L. *et al.* (2012) MORC2 signaling integrates phosphorylation-dependent, ATPase-coupled chromatin remodeling during the DNA damage response. *Cell Rep.*, **2**, 1657–1669.

22. Sevilla,T., Lupo,V., Martinez-Rubio,D., Sancho,P., Sivera,R., Chumillas,M.J., Garcia-Romero,M., Pascual-Pascual,S.I., Muelas,N., Dopazo,J. *et al.* (2016) Mutations in the MORC2 gene cause axonal Charcot-Marie-Tooth disease. *Brain*, **139**, 62–72.

23. Ando,M., Okamoto,Y., Yoshimura,A., Yuan,J.H., Hiramatsu,Y., Higuchi,Y., Hashiguchi,A., Mitsui,J., Ishiura,H., Fukumura,S. *et al.* (2017) Clinical and mutational spectrum of Charcot-Marie-Tooth disease type 2Z caused by MORC2 variants in Japan. *Eur. J. Neurol.*, **24**, 1274–1282.

24. Albulym,O.M., Kennerson,M.L., Harms,M.B., Drew,A.P., Siddell,A.H., Auer-Grumbach,M., Pestronk,A., Connolly,A., Baloh,R.H., Zuchner,S. *et al.* (2016) MORC2 mutations cause axonal Charcot-Marie-Tooth disease with pyramidal signs. *Ann. Neurol.*, **79**, 419–427.

25. Sancho,P., Bartesaghi,L., Miossec,O., Garcia-Garcia,F., Ramirez-Jimenez,L., Siddell,A., Akesson,E., Hedlund,E., Lassuthova,P., Pascual-Pascual,S.I. *et al.* (2019) Characterization of molecular mechanisms underlying the axonal Charcot-Marie-Tooth neuropathy caused by MORC2 mutations. *Hum. Mol. Genet.*, **28**, 1629–1644.

26. Zhang,F.L., Cao,J.L., Xie,H.Y., Sun,R., Yang,L.F., Shao,Z.M. and Li,D.Q. (2018) Cancer-associated MORC2-mutant M276I regulates an hnRNPM-mediated CD44 splicing switch to promote invasion and metastasis in triple-negative breast cancer. *Cancer Res.*, **78**, 5780–5792.

27. Perry,J. and Zhao,Y. (2003) The CW domain, a structural module shared amongst vertebrates, vertebrate-infecting parasites and higher plants. *Trends Biochem. Sci.*, **28**, 576–580.

28. He,F., Umehara,T., Saito,K., Harada,T., Watanabe,S., Yabuki,T., Kigawa,T., Takahashi,M., Kuwasako,K., Tsuda,K. *et al.* (2010) Structural insight into the zinc finger CW domain as a histone modification reader. *Structure*, **18**, 1127–1139.

29. Hoppmann,V., Thorstensen,T., Kristiansen,P.E., Veiseth,S.V., Rahman,M.A., Finne,K., Aalen,R.B. and Aasland,R. (2011) The CW domain, a new histone recognition module in chromatin proteins. *EMBO J.*, **30**, 1939–1952.

30. Liu,Y., Tempel,W., Zhang,Q., Liang,X., Loppnau,P., Qin,S. and Min,J. (2016) Family-wide characterization of histone binding abilities of human CW domain-containing proteins. *J. Biol. Chem.*, **291**, 9000–9013.

31. Ding,Q.S., Zhang,L., Wang,B.C., Zeng,Z., Zou,X.Q., Cao,P.B., Zhou,G.M., Tang,M., Wu,L., Wu,L.L. *et al.* (2018) Aberrant high expression level of MORC2 is a common character in multiple cancers. *Hum. Pathol.*, **76**, 58–67.

32. Pan,Z., Ding,Q., Guo,Q., Guo,Y., Wu,L., Wu,L., Tang,M., Yu,H. and Zhou,F. (2018) MORC2, a novel oncogene, is upregulated in liver cancer and contributes to proliferation, metastasis and chemoresistance. *Int. J. Oncol.*, **53**, 59–72.

33. Liu,J., Shao,Y., He,Y., Ning,K., Cui,X., Liu,F., Wang,Z. and Li,F. (2019) MORC2 promotes development of an aggressive colorectal cancer phenotype through inhibition of NDRG1. *Cancer Sci.*, **110**, 135–146.

34. Wang,T., Qin,Z.Y., Wen,L.Z., Guo,Y., Liu,Q., Lei,Z.J., Pan,W., Liu,K.J., Wang,X.W., Lai,S.J. *et al.* (2018) Epigenetic restriction of Hippo signaling by MORC2 underlies stemness of hepatocellular carcinoma cells. *Cell Death Differ.*, **25**, 2086–2100.

35. Liu,J., Zhang,Q., Ruan,B., Chen,W., Zheng,J., Xu,B., Jiang,P., Miao,Z., Li,F., Guo,J.Y. *et al.* (2019) MORC2 regulates C/EBPalpha-mediated cell differentiation via sumoylation. *Cell Death Differ.*, **26**, 1905–1917.

36. Zhang,L. and Li,D.Q. (2019) MORC2 regulates DNA damage response through a PARP1-dependent pathway. *Nucleic Acids Res.*, **47**, 8502–8520.

37. Gong,F., Chiu,L.Y. and Miller,K.M. (2016) Acetylation reader proteins: Linking acetylation signaling to genome maintenance and cancer. *PLoS Genet.*, **12**, e1006272.

38. Narita,T., Weinert,B.T. and Choudhary,C. (2019) Functions and mechanisms of non-histone protein acetylation. *Nat. Rev. Mol. Cell Biol.*, **20**, 156–174.

39. Choudhary,C., Weinert,B.T., Nishida,Y., Verdin,E. and Mann,M. (2014) The growing landscape of lysine acetylation links metabolism and cell signalling. *Nat. Rev. Mol. Cell Biol.*, **15**, 536–550.

40. Arango,D., Sturgill,D., Alhusaini,N., Dillman,A.A., Sweet,T.J., Hanson,G., Hosogane,M., Sinclair,W.R., Nanan,K.K., Mandler,M.D. *et al.* (2018) Acetylation of cytidine in mRNA promotes translation efficiency. *Cell*, **175**, 1872–1886.

41. Sharma,S., Langhendries,J.L., Watzinger,P., Kotter,P., Entian,K.D. and Lafontaine,D.L. (2015) Yeast Kre33 and human NAT10 are conserved 18S rRNA cytosine acetyltransferases that modify tRNAs assisted by the adaptor Tan1/THUMPD1. *Nucleic Acids Res.*, **43**, 2242–2258.

42. Ito,S., Horikawa,S., Suzuki,T., Kawauchi,H., Tanaka,Y., Suzuki,T. and Suzuki,T. (2014) Human NAT10 is an ATP-dependent RNA acetyltransferase responsible for N4-acetylcytidine formation in 18 S ribosomal RNA (rRNA). *J. Biol. Chem.*, **289**, 35724–35730.

43. Liu,X., Tan,Y., Zhang,C., Zhang,Y., Zhang,L., Ren,P., Deng,H., Luo,J., Ke,Y. and Du,X. (2016) NAT10 regulates p53 activation through acetylating p53 at K120 and ubiquitinating Mdm2. *EMBO Rep.*, **17**, 349–366.

44. Liu,X., Cai,S., Zhang,C., Liu,Z., Luo,J., Xing,B. and Du,X. (2018) Deacetylation of NAT10 by Sirt1 promotes the transition from rRNA biogenesis to autophagy upon energy stress. *Nucleic Acids Res.*, **46**, 9601–9616.

45. Shen,Q., Zheng,X., McNutt,M.A., Guang,L., Sun,Y., Wang,J., Gong,Y., Hou,L. and Zhang,B. (2009) NAT10, a nucleolar protein, localizes to the midbody and regulates cytokinesis and acetylation of microtubules. *Exp. Cell Res.*, **315**, 1653–1667.

46. Larrieu,D., Vire,E., Robson,S., Breusegem,S.Y., Kouzarides,T. and Jackson,S.P. (2018) Inhibition of the acetyltransferase NAT10

normalizes progeric and aging cells by rebalancing the Transportin-1 nuclear import pathway. *Sci. Signal*, **11**, eaar5401.

47. Balmus,G., Larrieu,D., Barros,A.C., Collins,C., Abrudan,M., Demir,M., Geisler,N.J., Lelliott,C.J., White,J.K., Karp,N.A. *et al.* (2018) Targeting of NAT10 enhances healthspan in a mouse model of human accelerated aging syndrome. *Nat. Commun.*, **9**, 1700.

48. Larrieu,D., Britton,S., Demir,M., Rodriguez,R. and Jackson,S.P. (2014) Chemical inhibition of NAT10 corrects defects of laminopathic cells. *Science*, **344**, 527–532.

49. Tschida,B.R., Temiz,N.A., Kuka,T.P., Lee,L.A., Riordan,J.D., Tierrablanca,C.A., Hullsiek,R., Wagner,S., Hudson,W.A., Linden,M.A. *et al.* (2017) Sleeping beauty insertional mutagenesis in mice identifies drivers of steatosis-associated hepatic tumors. *Cancer Res.*, **77**, 6576–6588.

50. Li,Q., Liu,X., Jin,K., Lu,M., Zhang,C., Du,X. and Xing,B. (2017) NAT10 is upregulated in hepatocellular carcinoma and enhances mutant p53 activity. *BMC Cancer*, **17**, 605.

51. Ma,R., Chen,J., Jiang,S., Lin,S., Zhang,X. and Liang,X. (2016) Up regulation of NAT10 promotes metastasis of hepatocellular carcinoma cells through epithelial-to-mesenchymal transition. *Am. J. Transl. Res.*, **8**, 4215–4223.

52. Li,F.L., Liu,J.P., Bao,R.X., Yan,G., Feng,X., Xu,Y.P., Sun,Y.P., Yan,W., Ling,Z.Q., Xiong,Y. *et al.* (2018) Acetylation accumulates PFKFB3 in cytoplasm to promote glycolysis and protects cells from cisplatin-induced apoptosis. *Nat. Commun.*, **9**, 508.

53. Sun,R., Xie,H.Y., Qian,J.X., Huang,Y.N., Yang,F., Zhang,F.L., Shao,Z.M. and Li,D.Q. (2018) FBXO22 Possesses both protumorigenic and antimetastatic roles in breast cancer progression. *Cancer Res.*, **78**, 5274–5286.

54. Ran,F.A., Hsu,P.D., Wright,J., Agarwala,V., Scott,D.A. and Zhang,F. (2013) Genome engineering using the CRISPR-Cas9 system. *Nat. Protoc.*, **8**, 2281–2308.

55. Yang,Y.L., Zhang,Y., Li,D.D., Zhang,F.L., Liu,H.Y., Liao,X.H., Xie,H.Y., Lu,Q., Zhang,L., Hong,Q. *et al.* (2020) RNF144A functions as a tumor suppressor in breast cancer through ubiquitin ligase activity-dependent regulation of stability and oncogenic functions of HSPA2. *Cell Death Differ.*, **27**, 1105–1118.

56. Liu,J., Zhang,C., Zhao,Y., Yue,X., Wu,H., Huang,S., Chen,J., Tomsky,K., Xie,H., Khella,C.A. *et al.* (2017) Parkin targets HIF-1alpha for ubiquitination and degradation to inhibit breast tumor progression. *Nat. Commun.*, **8**, 1823.

57. Scholz,C., Weinert,B.T., Wagner,S.A., Beli,P., Miyake,Y., Qi,J., Jensen,L.J., Streicher,W., McCarthy,A.R., Westwood,N.J. *et al.* (2015) Acetylation site specificities of lysine deacetylase inhibitors in human cells. *Nat. Biotechnol.*, **33**, 415–423.

58. Huang,K.Y., Lee,T.Y., Kao,H.J., Ma,C.T., Lee,C.C., Lin,T.H., Chang,W.C. and Huang,H.D. (2019) dbPTM in 2019: exploring disease association and cross-talk of post-translational modifications. *Nucleic Acids Res.*, **47**, D298–D308.

59. Xu,H., Zhou,J., Lin,S., Deng,W., Zhang,Y. and Xue,Y. (2017) PLMD: An updated data resource of protein lysine modifications. *J Genet Genomics*, **44**, 243–250.

60. Hornbeck,P.V., Zhang,B., Murray,B., Kornhauser,J.M., Latham,V. and Skrzypek,E. (2015) PhosphoSitePlus, 2014: mutations, PTMs and recalibrations. *Nucleic Acids Res.*, **43**, D512–D520.

61. Wang,L., Du,Y., Lu,M. and Li,T. (2012) ASEB: a web server for KAT-specific acetylation site prediction. *Nucleic Acids Res.*, **40**, W376–W379.

62. Choudhary,C., Kumar,C., Gnad,F., Nielsen,M.L., Rehman,M., Walther,T.C., Olsen,J.V. and Mann,M. (2009) Lysine acetylation targets protein complexes and co-regulates major cellular functions. *Science*, **325**, 834–840.

63. Beli,P., Lukashchuk,N., Wagner,S.A., Weinert,B.T., Olsen,J.V., Baskcomb,L., Mann,M., Jackson,S.P. and Choudhary,C. (2012) Proteomic investigations reveal a role for RNA processing factor THRAP3 in the DNA damage response. *Mol. Cell*, **46**, 212–225.

64. Elia,A.E., Boardman,A.P., Wang,D.C., Huttlin,E.L., Everley,R.A., Dephoure,N., Zhou,C., Koren,I., Gygi,S.P. and Elledge,S.J. (2015) Quantitative proteomic Atlas of ubiquitination and acetylation in the DNA damage response. *Mol. Cell*, **59**, 867–881.

65. Houtkooper,R.H., Pirinen,E. and Auwerx,J. (2012) Sirtuins as regulators of metabolism and healthspan. *Nat. Rev. Mol. Cell Biol.*, **13**, 225–238.

66. Sanchez-Solana,B., Li,D.Q. and Kumar,R. (2014) Cytosolic functions of MORC2 in lipogenesis and adipogenesis. *Biochim. Biophys. Acta*, **1843**, 316–326.

67. North,B.J., Marshall,B.L., Borra,M.T., Denu,J.M. and Verdin,E. (2003) The human Sir2 ortholog, SIRT2, is an NAD+-dependent tubulin deacetylase. *Mol. Cell*, **11**, 437–444.

68. Veith,S., Schink,A., Engbrecht,M., Mack,M., Rank,L., Rossatti,P., Hakobyan,M., Goly,D., Hefele,T., Frensch,M. *et al.* (2019) PARP1 regulates DNA damage-induced nucleolar-nucleoplasmic shuttling of WRN and XRCC1 in a toxicant and protein-specific manner. *Sci. Rep.*, **9**, 10075.

69. Liu,H., Ling,Y., Gong,Y., Sun,Y., Hou,L. and Zhang,B. (2007) DNA damage induces N-acetyltransferase NAT10 gene expression through transcriptional activation. *Mol. Cell. Biochem.*, **300**, 249–258.

70. Manni,I., Mazzaro,G., Gurtner,A., Mantovani,R., Haugwitz,U., Krause,K., Engeland,K., Sacchi,A., Soddu,S. and Piaggio,G. (2001) NF-Y mediates the transcriptional inhibition of the cyclin B1, cyclin B2, and cdc25C promoters upon induced G2 arrest. *J. Biol. Chem.*, **276**, 5570–5576.

71. Davis,F.M., Tsao,T.Y., Fowler,S.K. and Rao,P.N. (1983) Monoclonal antibodies to mitotic cells. *Proc. Natl. Acad. Sci. U.S.A.*, **80**, 2926–2930.

72. Crosby,M.E., Jacobberger,J., Gupta,D., Macklis,R.M. and Almasan,A. (2007) E2F4 regulates a stable G2 arrest response to genotoxic stress in prostate carcinoma. *Oncogene*, **26**, 1897–1909.

73. Yan,Y., Hein,A.L., Greer,P.M., Wang,Z., Kolb,R.H., Batra,S.K. and Cowan,K.H. (2015) A novel function of HER2/Neu in the activation of G2/M checkpoint in response to gamma-irradiation. *Oncogene*, **34**, 2215–2226.

74. Peng,A. and Chen,P.L. (2003) NFBD1, like 53BP1, is an early and redundant transducer mediating Chk2 phosphorylation in response to DNA damage. *J. Biol. Chem.*, **278**, 8873–8876.

75. Mir,S.E., De Witt Hamer,P.C., Krawczyk,P.M., Balaj,L., Claes,A., Niers,J.M., Van Tilborg,A.A., Zwinderman,A.H., Geerts,D., Kaspers,G.J. *et al.* (2010) In silico analysis of kinase expression identifies WEE1 as a gatekeeper against mitotic catastrophe in glioblastoma. *Cancer Cell*, **18**, 244–257.

76. Tuupanen,S., Hanninen,U.A., Kondelin,J., von Nandelstadh,P., Cajuso,T., Gylfe,A.E., Katainen,R., Tanskanen,T., Ristolainen,H., Bohm,J. *et al.* (2014) Identification of 33 candidate oncogenes by screening for base-specific mutations. *Br. J. Cancer*, **111**, 1657–1662.

77. Black,J.C., Mosley,A., Kitada,T., Washburn,M. and Carey,M. (2008) The SIRT2 deacetylase regulates autoacetylation of p300. *Mol. Cell*, **32**, 449–455.

78. Eskandarian,H.A., Impens,F., Nahori,M.A., Soubigou,G., Coppee,J.Y., Cossart,P. and Hamon,M.A. (2013) A role for SIRT2-dependent histone H3K18 deacetylation in bacterial infection. *Science*, **341**, 1238858.

79. Dantuma,N.P. and van Attikum,H. (2016) Spatiotemporal regulation of posttranslational modifications in the DNA damage response. *EMBO J.*, **35**, 6–23.

80. Zhang,X., Chen,J., Jiang,S., He,S., Bai,Y., Zhu,L., Ma,R. and Liang,X. (2019) N-Acetyltransferase 10 enhances doxorubicin resistance in human hepatocellular carcinoma cell lines by promoting the Epithelial-to-Mesenchymal transition. *Oxid. Med. Cell Longev.*, **2019**, 7561879.

81. Wu,J., Zhu,H., Wu,J., Chen,W. and Guan,X. (2018) Inhibition of N-acetyltransferase 10 using remodelin attenuates doxorubicin resistance by reversing the epithelial-mesenchymal transition in breast cancer. *Am. J. Transl. Res.*, **10**, 256–264.